UNIVERSITY OF OKLAHOMA

GRADUATE COLLEGE

POST-MIGRATION SEISMIC DATA CONDITIONING METHODS ON A MERGED

DATASET

A THESIS

SUBMITTED TO THE GRADUATE FACULTY

in partial fulfillment of the requirement for the

Degree of

MASTER OF SCIENCE

By

PAMELA BLANCO DUFAU

Norman, Oklahoma

2024

POST-MIGRATION SEISMIC DATA CONDITIONING METHODS ON A MERGED

DATASET

A THESIS APPROVED FOR THE

SCHOOL OF GEOSCIENCES

BY THE COMMITTEE CONSISTING OF

Dr. Heather Bedle, Chair

Dr. Brett M. Carpenter

Dr. Matthew Pranter

Dedicated to all those who endeavor to improve themselves through education.

I hope it offers you some motivation and encouragement.

ACKNOWLEDGMENTS

This thesis was made possible by the support and trust of many people and institutions. First, thanks to the Fulbright program for seeing my potential and helping me with financial support to achieve my dream of studying abroad to further develop my skillset as a geoscientist.

I extend boundless gratitude to Dr. Heather Bedle, whose unwavering belief in me, encouragement to strive for excellence, and kindness during challenging times have been indispensable. These two years have been a journey of growth and learning, and I owe a part of my success to the AASPI team. Their assistance in adapting to a new culture, navigating coursework, and offering technical expertise has been invaluable. Special acknowledgment is reserved for Dr. Kurt Marfurt, whose mentorship imparted not only lessons in geophysics but also in the essence of humility in the professional realm.

I am also grateful to the faculty and staff of the School of Geosciences for providing invaluable advice throughout my journey. I also acknowledge the generosity of the Giddens family, particularly Mr. Brent, for sharing your lovely memories with me.

To my family, lifelong friends, my new lifelong friends, and my love, thank you for being the most important support in this adventure. Your long talks, encouragement, and confidence in me have been invaluable, and I am truly grateful that each of you is part of my life.

Lastly, thanks to the public, high-quality, and free education from my beloved country, Argentina. I am a daughter of public education, and I will forever advocate for it so more people like me can have the opportunity to live a better life through high-level education. I will be forever thankful to public education for giving me the tools that brought me to write these lines.

CONTENTS

VIII

LIST OF FIGURES

LIST OF TABLES

ABSTRACT

Analyzing amplitude anomalies in seismic data requires a comprehensive understanding of the geological context and the accuracy of the seismic image to faithfully represent the subsurface. Over the past four decades, numerous surveys in mature basins like the US Gulf of Mexico have undergone reprocessing and merging to enhance imaging quality. While this reprocessing primarily aims to optimize imaging for historical targets, it may yield suboptimal results for current objectives, such as identifying and characterizing shallow targets mandated by government regulations to prevent oil blowouts.

The merging of seismic data volumes demands careful attention during processing, as the different volumes are often acquired at different times with different hardware, acquisition geometries, and exploration objectives. If insufficient care is taken, significant differences in the amplitude and spectra of the merged survey components can pose challenges when used as input for machine learning techniques or seismic attribute studies.

To address discrepancies in the Matagorda Island merged survey, we implemented spectral balancing followed by structure-oriented filtering. Spectral balancing equalizes high and low frequencies, creating a more uniform frequency spectrum. Structure-oriented filtering eliminates random and cross-cutting coherent noise while preserving structural and stratigraphic features. This workflow ameliorates the discrepancies between the areas covered by the individual surveys, resulting in a more consistent interpretation across the seam between the two surveys. However, the application of this workflow posed a challenge in improving features observed at the tuning frequency and also exacerbating the high-frequency noise due to the presence of footprint, thus resulting in a more challenging interpretation of faults and fractures in some areas.

POST-MIGRATION SEISMIC DATA CONDITIONING METHODS ON A MERGED DATASET

INTRODUCTION

In the past years, merging legacy seismic surveys, shot with different acquisition parameters and at different times, has provided an advantage for the industry in covering extensive areas in a single cube. Morse and Spear (2022) explain the benefits that companies have by merging different datasets to obtain a single megamerge. They point out the advantage of obtaining a regional and sedimentological context. Additionally, they state that companies have a clear economic benefit since they can now review farm-in opportunities before third-party discussions, this means that a company can evaluate the technical, financial, and strategic risks before acquiring a percentage of an exploration block. Del Moro et al. (2013) showed the advantages of merging cubes for obtaining regional stratigraphic interpretations. Their research demonstrated how an appropriate selection of migration aperture can aid in visualizing sharper and higher-resolution features. However, the merging process requires special attention when matching amplitudes, frequencies, and phases from the different cubes. The result of an inaccurate merging process can lead to inconsistencies in the seismic data and erroneous geologic interpretations. Under this scenario, a new acquisition or data reprocessing to fix those issues might be complicated or even impossible. For this reason, handling post-migration filters to enhance the data quality becomes paramount when dealing with low-quality seismic datasets.

To investigate the use of post-migration workflows to improve the interpretation of merged datasets with visible differences along their seams and low resolution, we use a seismic dataset that is the product of merging two legacy surveys acquired at different times and with different acquisition parameters. We observe a sharp contrast in amplitudes and frequencies at the seam of the two original cubes and a strong presence of noise and artifacts from the processing (Figure 1).

We propose the application of a post-migration seismic data conditioning workflow consisting of applying spectral balancing followed by structure-oriented filtering. We first explore the use of spectral balancing to reduce the sharp contrast at the seam by homogenizing the frequency values and minimizing the sharp contrast generated during the merging process. Tufeckcik et al. (1981) state that a set of traces is spectrally balanced when they have the same frequency spectrum that the filter applied for spectral balance. The interpreter should generally compute a survey-consistent spectral balancing whereby the same time-variant filter is applied to the entire volume, thereby preserving lateral changes and relative amplitudes (Chopra and Marfurt, 2016). However, as we are dealing with a merged dataset in which the two legacy surveys had different but relatively consistent amplitude and frequency spectra, the approach of an amplitude-friendly survey-consistent correction would not have shown any improvement in reducing the sharp contrast at the seam. As an alternative, we applied trace-by-trace spectral balancing, which treats each trace independently and attempts to generate a balanced spectrum across the entire survey. In our implementation, because we used a long-time window, spectral balancing preserves the relative amplitude of each trace in a statistically reasonable manner and reduces the frequency contrast across the merged cube. Following the trace-by-trace spectral balancing of the dataset, we applied structure-oriented filtering (SOF). This process attempts to improve the visualization of

2

structural and stratigraphic edges (Marfurt, 2018). Its application in this stage aims to highlight features that were unraveled in the previous step.

In this work, we evaluate the above-mentioned post-migration techniques applied independently on the original merged dataset and then combined. We present the effect of these filters on the homogenization of frequencies and amplitudes distribution across the seam and the enhancement of seismic resolution, as well as their benefit or damage to the interpretation of structural and stratigraphic features. We also discuss the application of automatic gain control (AGC) to address the amplitude mismatch due to merging issues and how the variation in the parameters for their application may impact the identification of direct hydrocarbon indicators.

SEISMIC DATA

The Matagorda Island block is located on the continental shelf of Texas (Figure 1-a). The area is located 60 mi NW of Corpus Christi, approximetly10 mi from the coastline. The seismic data from the block covers an area of 1,080 mi^2. This merge seismic cube exhibits varying seismic expressions due to reprocessing issues and low signal-to-noise ratio (SNR) caused by footprints (Figure 1-e). For this work, we selected a ~100 km^2 portion of the block, in which there is a visible amplitude and frequency change due to the merging of two different surveys (Figure 1-d).
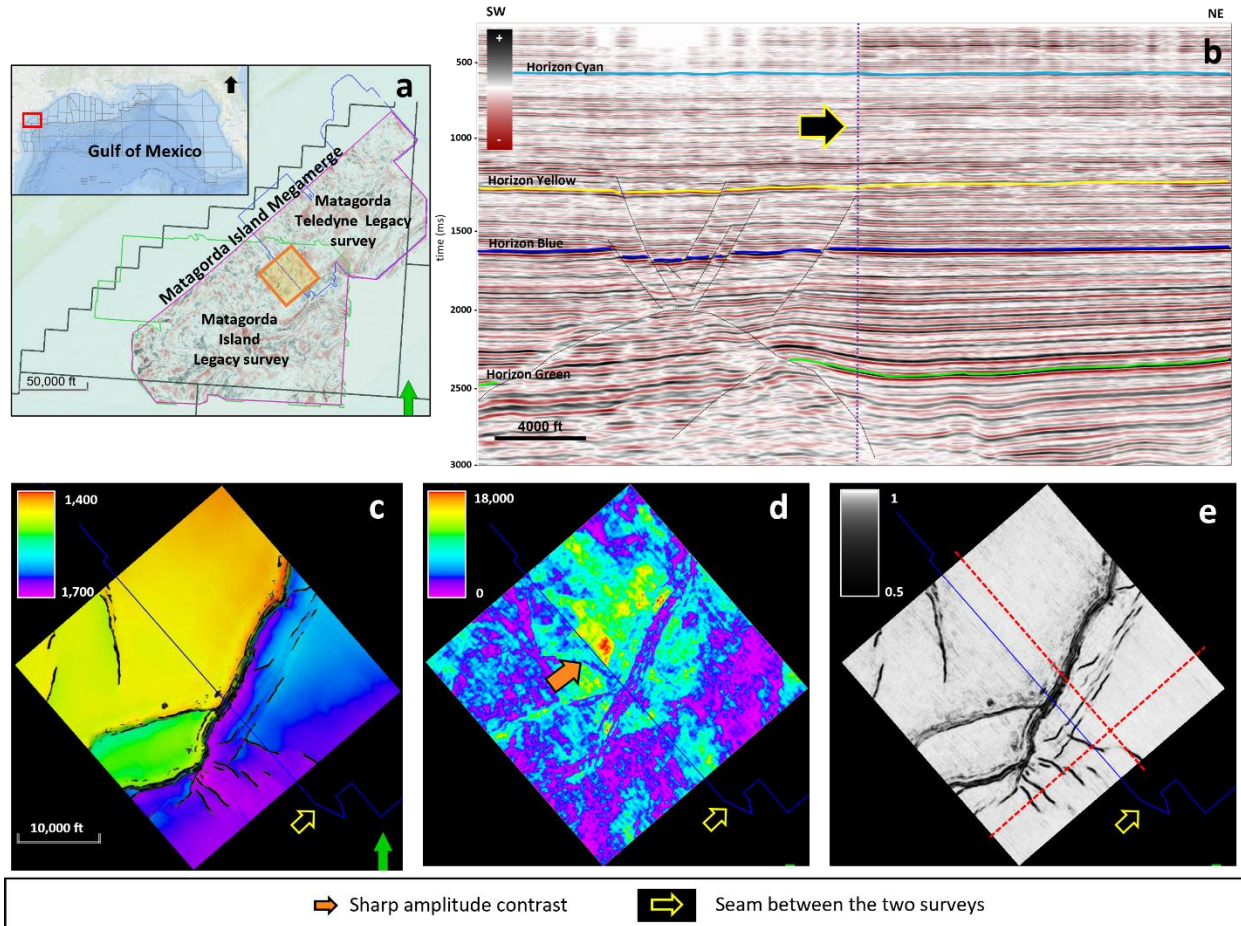
Figure 1. *a) Seismic dataset location within the Gulf of Mexico. The time slice shows the extent of the Matagorda Island megamerge dataset, while the blue and green polygons represent the extent of the legacy surveys. The orange polygon represents the portion of volume used in this study; b) representative crossline of the area of interest of this project; c) structural map (TWT) of the seismic horizon used to analyze the impact of conditioning methods on this study; d) time slice displaying the sharp amplitude contrast at both sides of the seam using envelope attribute; and e) Sobel filter map over Horizon Blue displaying in detail the faulting system of the area. The red dashed lines represent the orientation of the inlines (NW-SE), and crosslines (SW-NE) used in this project.*

Figure 1-c displays the structural map in time (TWT) of Horizon Blue, the reflector used to analyze attributes in the following sections. On this map, warm colors represent the shallowest areas of the reflector, while cold colors represent the deepest. We can notice that the horizon is majorly affected by a normal fault striking in the NW-SE direction. This fault has been interpreted

4

as the Clemente-Tomas fault in the area of study (Figure 2). Additionally, Horizon Blue is affected by secondary faults (Figure 1e). These minor faults play a key role in evaluating how seismic conditioning methods enhance the visualization of structures.
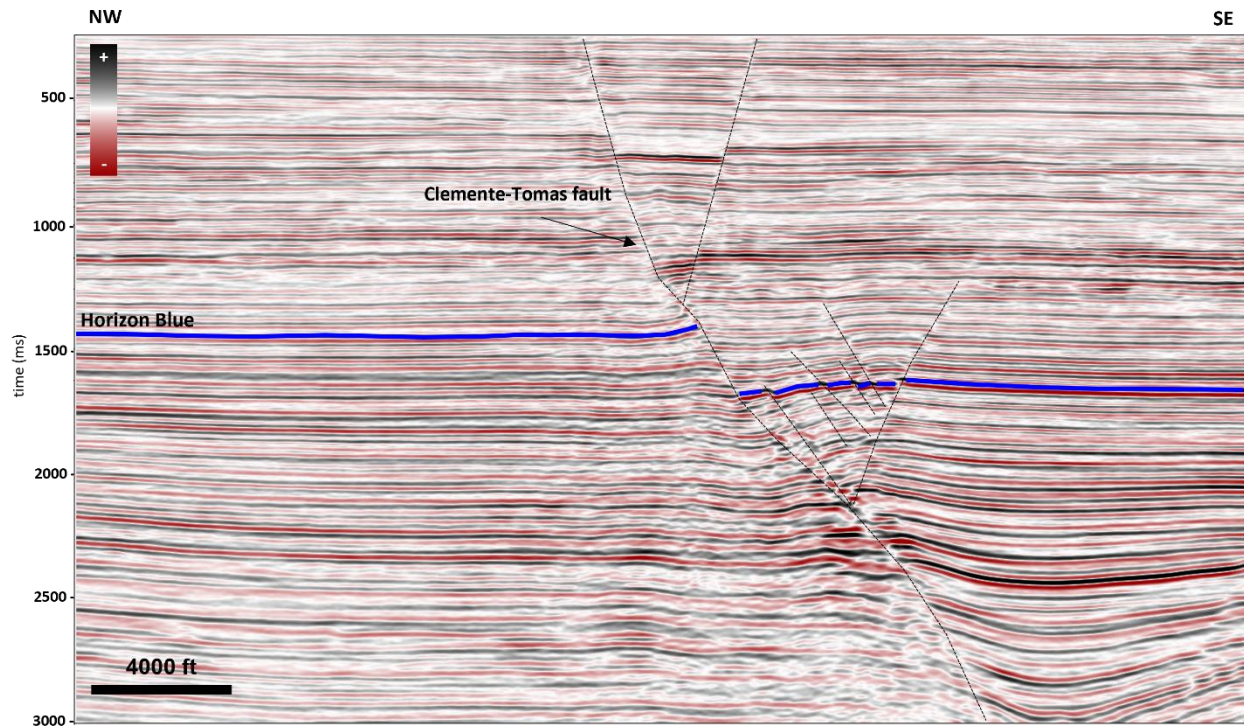
Figure 2. *Seismic inline through the Matagorda Island dataset used in this project. The interpretation in blue represents Horizon Blue, and the black-dotted lines represent the faults in the area. The main fault dipping to the SE direction is the Clemente-Tomas fault. The location of this crossline is referenced in Figure 1.*

The Matagorda Island Megamerge is the result of merging the Matagorda Teledyne and Matagorda Island surveys (Figure 1a).

Table 1 summarizes the available information about some of the acquisition parameters and documents the difference between them.

	Matagorda Island	Matagorda Teledyne
Vintage	May 1994	January 1991
Bin size	12.5 x 40 m	12.5 x 37.5 m
Number of channels	162	120
Fold	40	30
Channel spacing	25 m	25 m
Far offset	4000 m	3000 m
Number of cables	3	1
SP interval	50 m	25 m

Table 1. *Legacy surveys comparative chart.*

GEOLOGICAL SETTING AND STRATIGRAPHY

The main objective of this project is to investigate post-migration seismic data conditioning workflows on a merged dataset that presents amplitude and frequency changes at the seam of the legacy surveys and a poor resolution of stratigraphic features and fault structures. The geophysical evaluation of the dataset requires to anchor our understanding within the geological context of the western Gulf of Mexico. This region is characterized by significant faulting events and fluctuations in sedimentation patterns. Understanding this context is not only integral but foundational for the interpretation of seismic data. The geological background provides critical insights into the structural complexities and sedimentary sequences that exist in the subsurface.

Regional geology

The Gulf of Mexico is an ocean basin located between the North American plate and the Yucatan block. It was created during crustal extension and seafloor spreading in the Mesozoic Pangea breakup (Galloway, 2008). During a long period of Late Triassic to Early Jurassic, a series

of basement grabens and half-grabens were filled with terrestrial and volcaniclastic sediments. Most of the structural basin underlies a transitional crust that was stretched by Middle to Late Jurassic rifting. A remarkable event for the latter structural development of the basin is the continued stretching in Bathonian and Callovian times. During this episode, a broad sag was initiated, and the basin was opened to the Pacific Ocean, leading to the deposition of thick Louann Salt and associated evaporites (Galloway, 2008). The end of the Early Cretaceous determined the modern morphology of the Gulf Basin, in which the main processes were the combination of subsidence and carbonate platform deposition. After this, loading subsidence was the predominant mechanism in the Late Cretaceous, complicated by intrabasinal gravity tectonics structures (Galloway, 2008). Sea-level fluctuations in the Pleistocene have mainly controlled the morphology of the current continental shelves. The categories that can be assigned to the depositional environments on the continental shelf are generally terrigenous on the northern and western shelf and carbonate on the eastern edge. This pattern can be seen from the Late Cretaceous when the sediments were delivered to the northern margin of the Gulf from the continental interiors that were tectonically elevated. These sediments then prograded to the present shelf edge, covering a distance of about 300 km from the margin of the Cretaceous platform (Coleman et al., 1986). The Gulf of Mexico depocenter presents a thick column formed by a succession of sediments from the Jurassic to the Holocene periods (Galloway, 2008).

Local geology

Stratigraphy

Regarding the geology in the offshore Texas shelf, Coleman et al. (1986) described it as a broad area that currently displays a smooth topographic relief. The thin layer of sediments from the Holocene overlies an eroded subaerial fluvial plain from the Late Pleistocene that often crops

out on the sea floor. This area of the shelf presents infilled deep-seated channels. The Texas shelf edge displays a series of prograded Late Pleistocene deltas formed during the lowering of the sea level (Coleman et al., 1986). The sediments in this basin zone are mainly constituted by sand-shale interlayers that have been affected by listric faults detaching within a basal shale unit that typically dips basinward (Bose and Mitra, 2012). According to Spencer and Barrett (2007), the productive reservoirs from the neighboring area, Mustang Island, are composed of distal barrier-shoreface and shelf sands and thick fluvial-deltaic sands reworked in the strike direction and belong to the Frio Formation. This section represents a significant tertiary progradational wedge within the Texas Gulf coastal plain. The sedimentary materials forming this unit primarily originated from Mexico and the southwestern United States, resulting from uplift and erosion initiated in Mexico. This process was subsequently followed by uplift and erosion along the western margin of the Gulf basin (Swanson and Karlsen, 2009). The Frio Formation underlies the Oligocene Anahuac Formation, a transgressive marine shale in Texas and Louisiana. Anahuac consists of light- to dark-greenish-gray calcareous shale interbedded with thin beds of locally calcareous sandstone and locally thin limestones, becoming more calcareous from west to east (Swanson and Karlsen, 2009). Interbedded shales and calcareous sandstones are typical of middle shelf-intermediate open marine environments. Desselle (1997) stated that progradational distal delta-front sandstones, shoreface, and shelf sandstones of the Anahuac formation occur in offshore Texas's Matagorda Island and Mustang Island areas. Figure 3 shows a regional stratigraphic section of the Tertiary and younger strata in the northern Gulf of Mexico coastal plain (Swanson and Karlsen, 2009).

PERIOD	EPOCH	AGE	Rio Grande Embayment San Marcos Arch East Texas Basin (Texas)	Southeast Texas South Louisiana and Offshore (Texas & Louisiana)	Southeast Mississippi Southwest Alabama West Florida Panhandle and Offshore
QUAT.	HOLOC.		- - - -	- - - -	- - - -
	PLEIS.	Calabrian	Undifferentiated	Undifferentiated	Undifferentiated
NEOGENE	PLIOCENE	Piacenzian / Zanclean	Undifferentiated	Undifferentiated	Undifferentiated
	MIOCENE	Messinian / Tortonian	Goliad Fm.		Pascagoula Fm. Hattiesburg/Pensacola Fms. Catahoula Fm.
		Serravallian / Langhian	Lagarto Fm.	Fleming Fm.	
		Burdigalian / Aquitanian	Fleming Fm.		
TERTIARY / PALEOGENE	OLIGOCENE	Chattian	Catahoula/ Frio Fms. (Anahuac Fm.)	Catahoula/ Frio Fms. (Anahuac Fm., Hackberry)	Paynes Hammock Fm. Chickasawhay Fm.
		Rupelian	Vicksburg Group	Vicksburg Group	Vicksburg Group
	EOCENE	Priabonian	Jackson Group	Jackson Group	Jackson Group
		Bartonian / Lutetian	Claiborne Group	Claiborne Group	Claiborne Group
		Ypresian	Wilcox Group	Wilcox Group	Wilcox Group
	PAL.	Thanetian / Selandian / Danian	Midway Group	Midway Group	Midway Group

Figure 3. Expanded stratigraphic section of the youngest sediments in the northern Gulf of Mexico area. The Rio Grande Embayment, San Marcos Arch, East Texas Basin (Texas) column represents the zone of interest of this project. The blue rectangle represents the time in which we consider Horizon Blue was deposited according to Worrall and Snelson (1989). Chart modified from Swanson and Karlsen (2009).

Structural geology: the Clemente-Tomas fault

Growth fault systems in offshore Texas present four major fault trends (Bradshaw and Watkins, 1994). All of them are characterized by a northeast-southwest strike with a counterclockwise rotation in the southern area (Figure 4). The sediments in the Matagorda Island block are affected mainly by the Clemente-Tomas trend (Rangin et al., 2008). This early Miocene fault system lies basinward beneath the present inner-shelf surface (Bradshaw and Watkins, 1994). Bally and Palmer (1989) explain that the faults in this area are not simply basinward slumps and mention that the role of gravity in the development of these fault systems must be studied alongside

the complex geology of the slope region. McDonnell et al. (2010) described the geometry of the Clemente-Tomas fault in detail. In their work, they named this fault as the Miocene Detachment since it is a gravity-driven extensional faulting that resulted from gravity spreading due to salt migration during that period of time. Additionally, they presented evidence that this major growth fault presents an irregular geometry that is smooth landwards but gets corrugated seaward, alternating between highs and lows. Although previous literature (Bradshaw and Watkins, 1994; Bally and Palmer, 1989) argue that the Clemente-Tomas fault is a primarily shale-based detachment fault, McDonnell et al. (2010) defend that these corrugations were controlled by the evacuation of allochthonous salt canopy inferred to be emplaced between the late Eocene and early Oligocene and started migrating in the Oligocene to Middle Miocene.
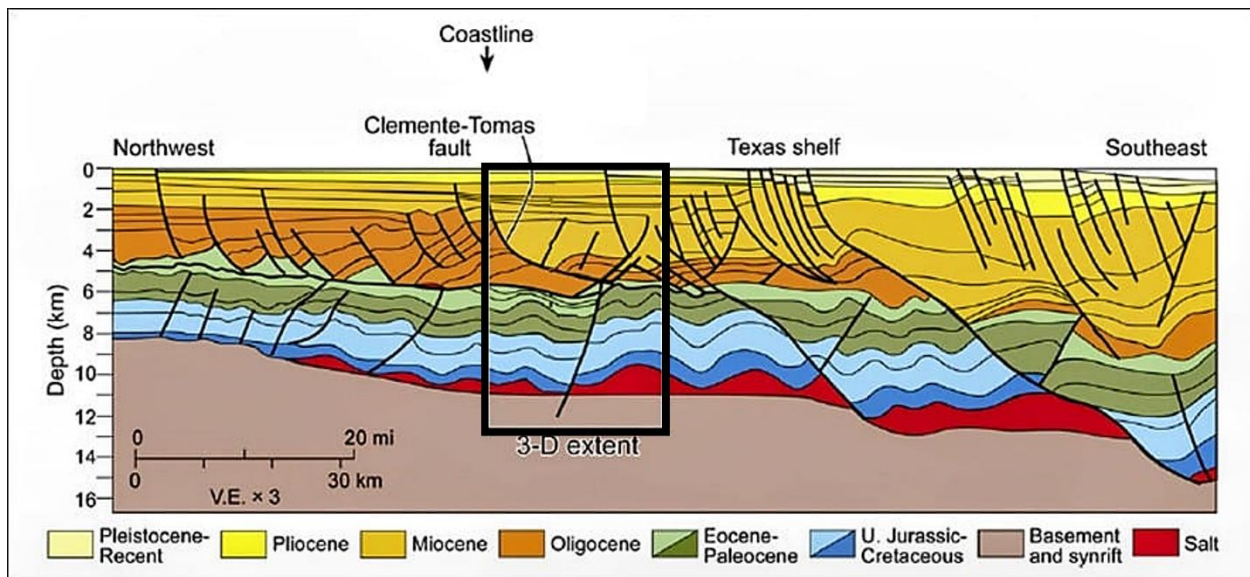
Figure 4. Regional profile across the study area. A regional detachment separates Oligo-Miocene extensional faults from deeper Cretaceous-Eocene sections. The interpreted horizons in this project are affected by the Clemente-Tomas fault. The black rectangle represents the extension of the Matagorda Island megamerge dataset. Figure modified from McDonnell et al., 2010.

METHODOLOGY

In assessing the merged survey data quality, we first mapped major horizons and then sliced through the amplitude and attribute volumes. This step entails evaluating the data, looking for discontinuities, and examining lateral variations in bandwidth and signal-to-noise (SNR) along the selected horizons. Figure 5 shows a simplified overview of the workflow followed in this project.
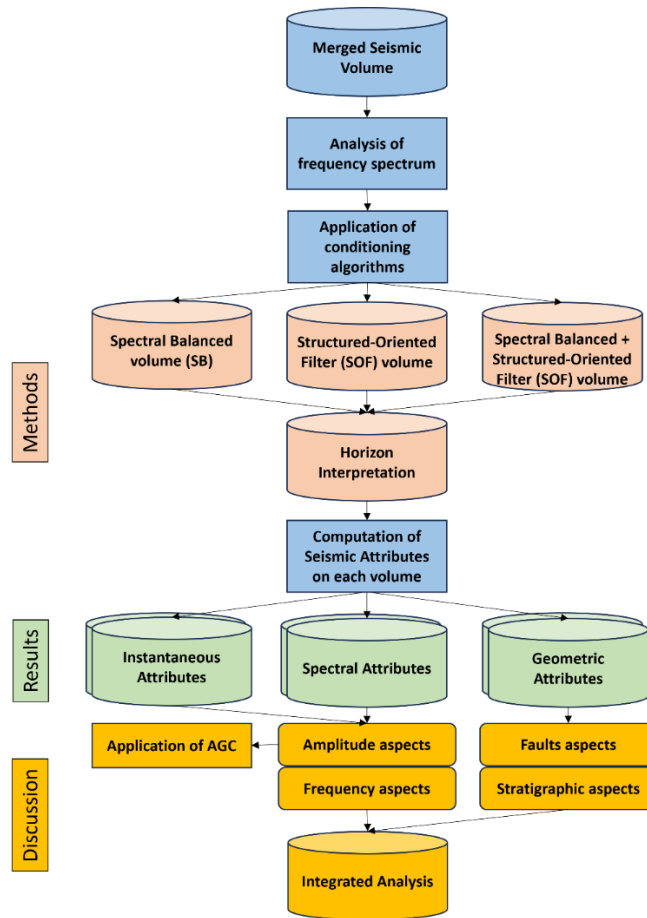
Figure 5. Project methodology and workflow for seismic data conditioning, attributes calculation, and discussion.

The core issue in the merged survey is displayed in Figure 6 and Figure 7, where we are displaying the cropped volume used for this study. We can observe a sharp amplitude contrast

located at the same place in every interpreted horizon, which is more evident in shallower areas. In Figure 6, we can observe how the attribute envelope behaves on the four interpreted horizons. As interpreters, we may realize that the sharp amplitude contrast at the seam area happening at Horizon Cyan and Horizon Yellow, which are the shallowest horizons, are hard to explain with geological reasoning, so the more obvious reason for it might be the presence of a geophysical artifact. However, the seam becomes less obvious when going deeper, as seen in Horizon Blue and Horizon Green. At this stage, the interpreter may confuse the amplitude contrast with a direct hydrocarbon indicator (DHI), leading to an inaccurate interpretation of the geology. These observations on the seismic data show the importance of analyzing amplitude changes even when we are doing a regional evaluation of the data.

Figure 7 is a crossline that goes through the area and displays the amplitude contrast at both sides of the seam, represented by the vertical dashed line. Consistently with what we observed in the maps of Figure 6, the sharp contrast is more evident in the shallowest part and becomes less notorious at greater depths. This observation in amplitudes discrepancy may be rooted in the processing time of the surveys. It is possible that for the time of the merging, the exploration and development targets were located below the two seconds. Therefore, the efforts in matching amplitudes and frequencies were focused on those depths. In consequence, the shallowest reflectors of the seismic data have more notorious amplitude contrast at both sides of the seam between the legacy surveys.
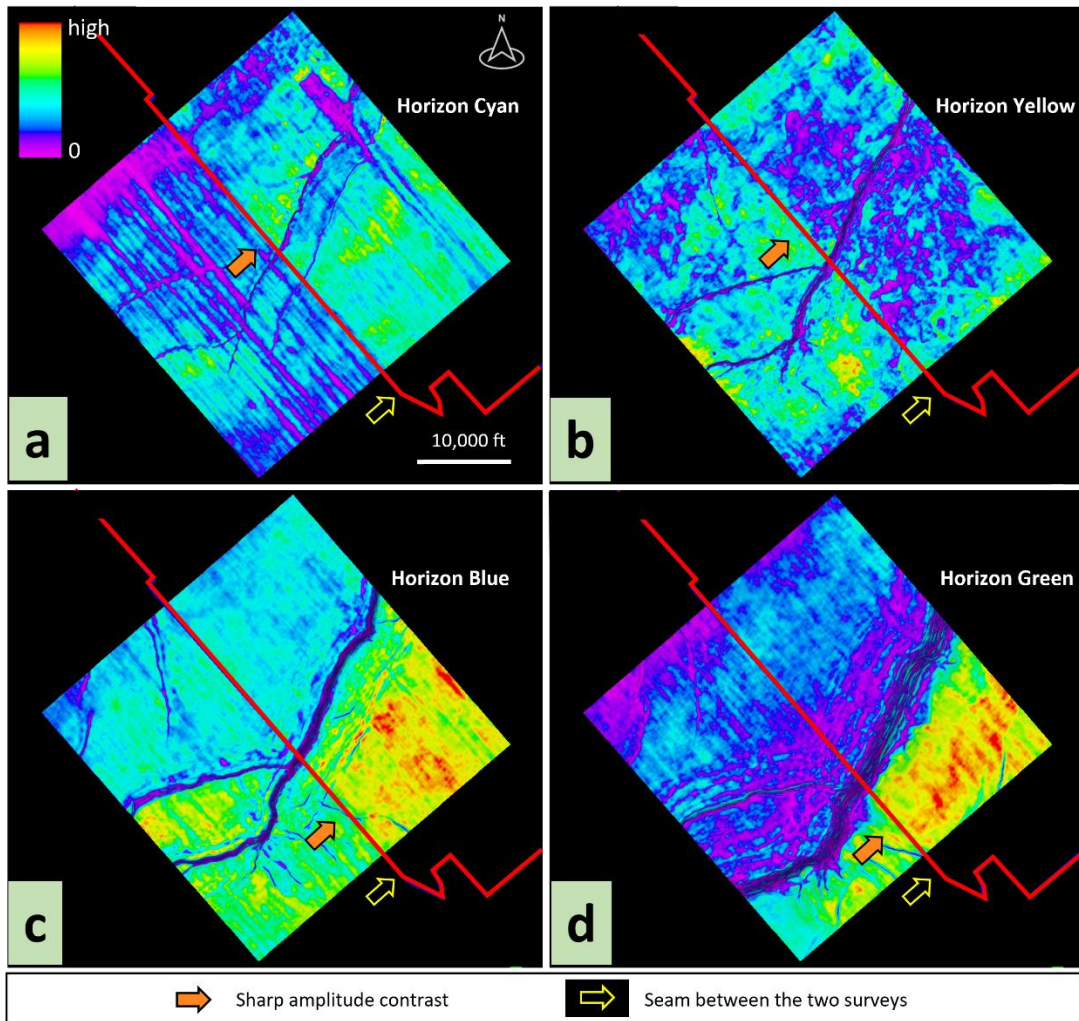
Figure 6. Horizon slices of a) Horizon Cyan, b) Horizon Yellow, c) Horizon Blue, and d) Horizon Green displaying the envelope attribute to focus on sharp amplitude contrast across the seam. The red line indicates the seam between the two legacy cubes. Note the footprint noise in the NW-SE direction.
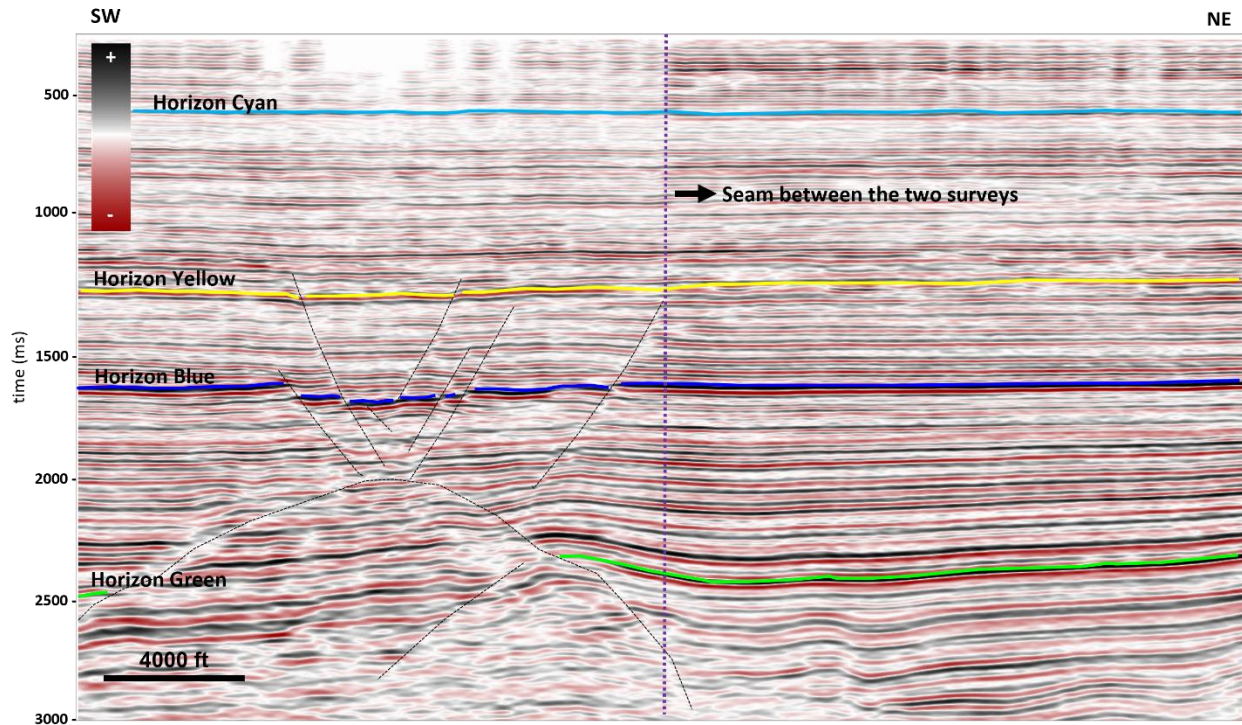
Figure 7. Seismic crossline through the original dataset showing the seam between the two surveys (vertical dotted line) and the horizons interpreted. Note the pronounced amplitude discrepancy at shallower levels. The location of this crossline is referenced in Figure 1.

Given these observations of amplitude variations within the merged dataset, it becomes necessary to attempt to improve the quality of the survey to ensure consistency of the interpretation. Here, we first address this problem by applying two postmigration data conditioning processes: spectral balancing and structure-oriented filtering. Additionally, we explore the impact of applying AGC in the amplitude contrast.

Several seismic attributes were calculated to evaluate the effect of the merge across the seam. The attributes calculated were envelope, instantaneous frequency, Sobel filter, total energy, mean frequency, and peak magnitude. Table 2 summarizes the types and applications of each attribute used in this analysis, and Appendix A further explains their physical principles.

Category	Attribute	Application	Examples
Single trace	Instantaneous Frequency	Identification of attenuation and thin-bed tuning.	Taner et al. (1979)
	Envelope	Sensitive to changes in acoustic impedance.	Taner et al. (1979)
Geometric	Sobel filter (similarity)	Stratigraphic edges and fault visualization.	Luo et al. (1996), Gersztenkorn and Marfurt (1999)
	Total Energy	Isolation of low energy chaotic reflectors from higher energy seismic responses.	Gersztenkorn and Marfurt (1999)
Spectral	Mean Frequency	Detection of thin-bed tuning anomalies.	Liu (2007), Marfurt (2018)
	Peak Magnitude	Strong hydrocarbon indicator.	Liu (2007), Marfurt (2018)

Table 2. *Summary of the attributes used in this study and their applications.*

Spectral Balancing

The seismic dataset used in this project presents heterogeneities in the seismic response due to an incorrect match of frequencies and amplitudes during the merging process. In this work, we address this problem by proposing a straightforward methodology, such as spectral balancing, to homogenize the seismic data at both sides of the seam of the merged cube and to enhance the frequency content of the volume. Marfurt (2018) stated that spectral balancing aims to relocate each spectral component to its ideal level. As we are working with frequencies, we must be aware of what is the original frequency spectrum of the data and not create frequencies that were never recorded. However, this methodology does not extend the range of frequencies by adding new

ones but enhances the existing frequencies by flattening the frequency spectrum in the usable range of frequencies.

Marfurt (2018) and Li et al. (2021) showed that if the input wavelet used to generate the seismic dataset is a Ricker wavelet, then after spectral balancing, the shape of the wavelet will have its side lobes reduced, meaning that the higher frequencies were improved. In other words, when we apply spectral balance, we aim to flatten the output wavelet spectra. The result of spectral balancing and enhancing high frequencies are reflected in a seismic output with more resolution, which, in practice, allows the interpreters to perform a detailed seismic interpretation.

The parameters used for spectral balancing were determined according to the spectral frequency analysis on the original seismic dataset. Figure 8 depicts the frequency spectrum of the cube before and after spectral balancing. We can observe that in the original cube, the usable frequencies are approximately 10 Hz to 40 Hz, with a dominant frequency around 20 Hz. After 40 Hz, we can see how frequency decays until it becomes almost zero at 70 Hz. The wavelet used to perform the spectral balancing was an Ormsby 5-10-75-85 Hz. We selected these wavelet parameters because we wanted to capture all the frequencies in the dataset. In addition, the dataset was examined in order to identify the more relevant frequencies and to recognize what frequencies are more contaminated with noise. Appendix B further explains the process of the spectral data analysis to get these frequency parameters for the Ormsby wavelet. Additionally, we applied the spectral balance on each trace individually. This method is chosen over a constant survey-wide spectral balancing because we have a merged cube with a mismatch of frequencies and amplitudes; herein, this approach attempts to generate a balanced spectrum across the entire survey. After applying spectral balance, we can observe the desired output of a flat frequency spectrum without a dominant frequency in Figure 8. The orange line represents the spectra of the volume after

spectral balancing. We observe that original amplitudes were reduced at certain frequency values, especially between 20 and 30 Hz. In addition, it is evident the frequency improvement above 40 Hz. The frequency spectrum shows that the dataset now has amplitude values for frequencies from 40 to 80 Hz. As we expected, no additional frequencies were created by applying spectral balance.

Structure-oriented filtering

In seismic interpretation, the interpreter must decide the most optimum tools to enhance the seismic data and highlight the target geologic features. Among the most common methods to conditionate a post-migrated dataset, structure-oriented filter (SOF) is well recognized to improve the imaging of the subsurface structures (Hocker and Fehmers, 2002; Luo et al., 2002; Hale, 2009; Marfurt, 2018).

In the case of the Matagorda Island dataset, which is a merged seismic cube that presents processing issues materialized as mismatching of amplitudes and frequencies at the seam of the legacy volumes and footprint noise in the NW-SE direction, we use this filter to improve the imaging quality and highlight small scale features that were revealed in the previous step when we applied spectral balance, and thus obtain an optimum visualization of both stratigraphic and structural features.

This filter is used to smooth the data while preserving the energy in the parallel direction to the structural dip. Additionally, it suppresses random noise and cross-cutting coherent noise. The SOF algorithm used in this study combines both Fehmers and Hoecker (2003) and Luo et al (2006) workflows for edge preservation but includes some other characteristics. Appendix C displays how this process impacts the data. The main difference between the algorithm performed in this project and the classic algorithms mentioned above is given by including a previously

computed similarity volume to measure the smoothness or edge presence and the possibility of choosing the type of filter applied to the data.

To apply this filter, we used a semblance cube (energy-ratio) to provide the algorithm with information about the structural geology and stratigraphic edges in the area of interest. The filter applied in this study is Principal Components, and it basically identifies consistent amplitude patterns that repeat sample by sample within an analysis window. The resultant frequency of the dataset, displayed in Figure 8 is practically the same as the input, meaning that this process does not change its amplitudes and frequencies. This is a desired effect when we need to enhance the visualization of stratigraphic and structural features without missing the amplitude and frequency information of the seismic events.

Cascaded spectral balancing and structure-oriented filtering

For this study, we want to evaluate the combination of two post-migration seismic data conditioning methods. Given the merged dataset with a mismatch of amplitudes and frequencies across the seam between the two legacy cubes, we first applied spectral balance to attempt to homogenize its distribution in that area and, after that, we applied SOF to enhance the visualization of stratigraphic edges that were revealed with spectral balancing. We first tried each method independently on the original dataset, evaluated the results separately, and finally combined them to improve the dataset's quality. The resultant frequency spectrum analysis is the same as that obtained by only applying spectral balance. This result is consistent with what we obtained in the previous section, where we saw that SOF does not modify any of those wave parameters. Figure 8 shows the frequency spectrum of all of the volumes analyzed in this work.
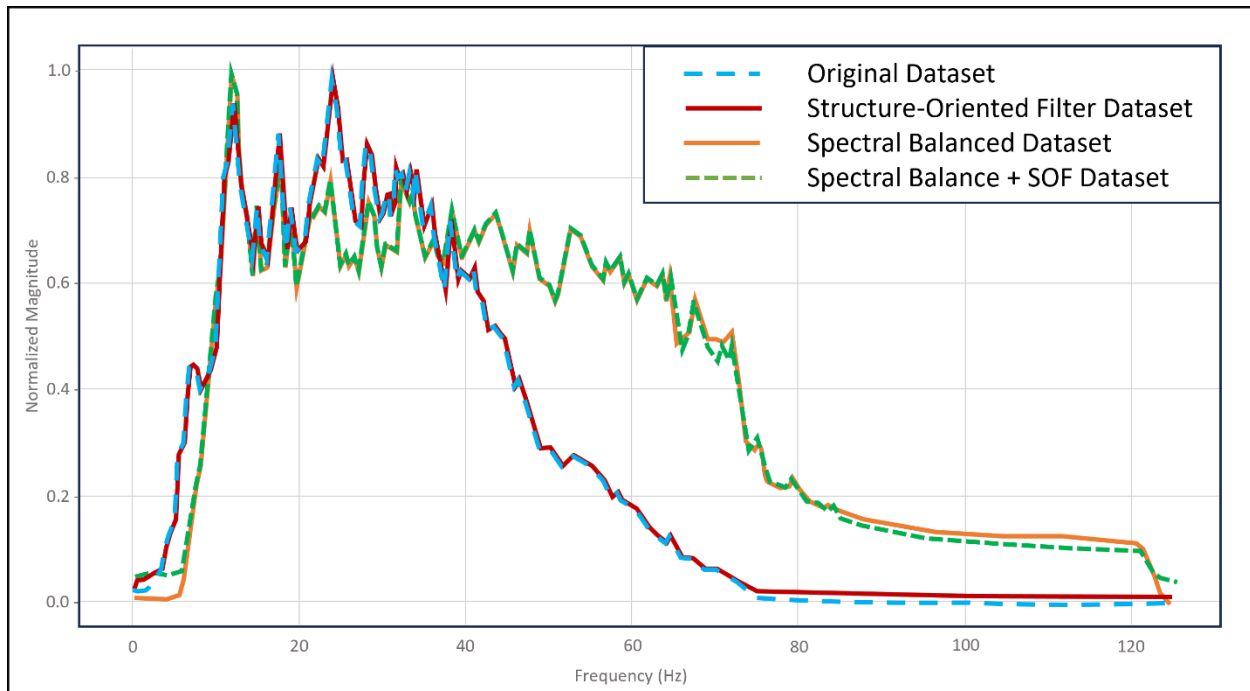
Figure 8. *Spectral frequency analysis of all of the volumes used in this project. Blue represents the original dataset, orange represents the spectrally balanced dataset, red represents the structure-oriented filtered dataset, and green represents the spectrally balanced and structure-oriented filtered dataset.*

RESULTS

We analyzed each method independently to understand how the post-migration processes impacted the Matagorda Island dataset. To do this, we compared each volume generated and analyzed their results. These cubes were the original post-stack time migration (PSTM), the spectrally balanced, the structure-oriented filtered (SOF), and the spectrally balanced and then structured-oriented filtered (SB + SOF) dataset. Figure 9 displays the interpretation of the seismic Inline 2200. In it we can see how the a) original data compares to the b) spectral balance, c) structure-oriented filter, and d) spectral balance and then structure-oriented filter. Since the inlines

are perpendicular to the main fault in the area, they are useful to observe the impact of the conditioning methods on the structures.

We can see the effect of spectral balancing in Figure 9-b by observing how the reflectors became more defined and how thin horizons are now easier to follow and pick. In addition, the maximum amplitudes were reduced from a value of 31,700 to 27,000, meaning a reduction of 15%. This reduction of amplitude values and reduction of relative amplitude contrast is a consequence of balancing each trace independently and requires special attention from the interpreter since it can affect the result of further seismic processes such as AVO or a seismic inversion.

After applying structure-oriented filtering on the original dataset, we can observe in Figure 9-c that the modification of the relative amplitudes is neglectable. As we expected from the theory, this method does not change the amplitudes and frequencies of the input. Consequently, we were not expecting to find a solution to the mismatch of amplitudes with SOF. Fault discontinuities are highlighted, making them easier to interpret and, in some cases, defining faults that were not visible in the original dataset.

The combination of both spectral balance and SOF in Figure 9-d shows a noticeable improvement compared to the original dataset (Figure 9-a). The most remarkable changes are the combination of what we observed in each method separately: reflectors more defined, better visualization of thin horizons, and better fault visualization.
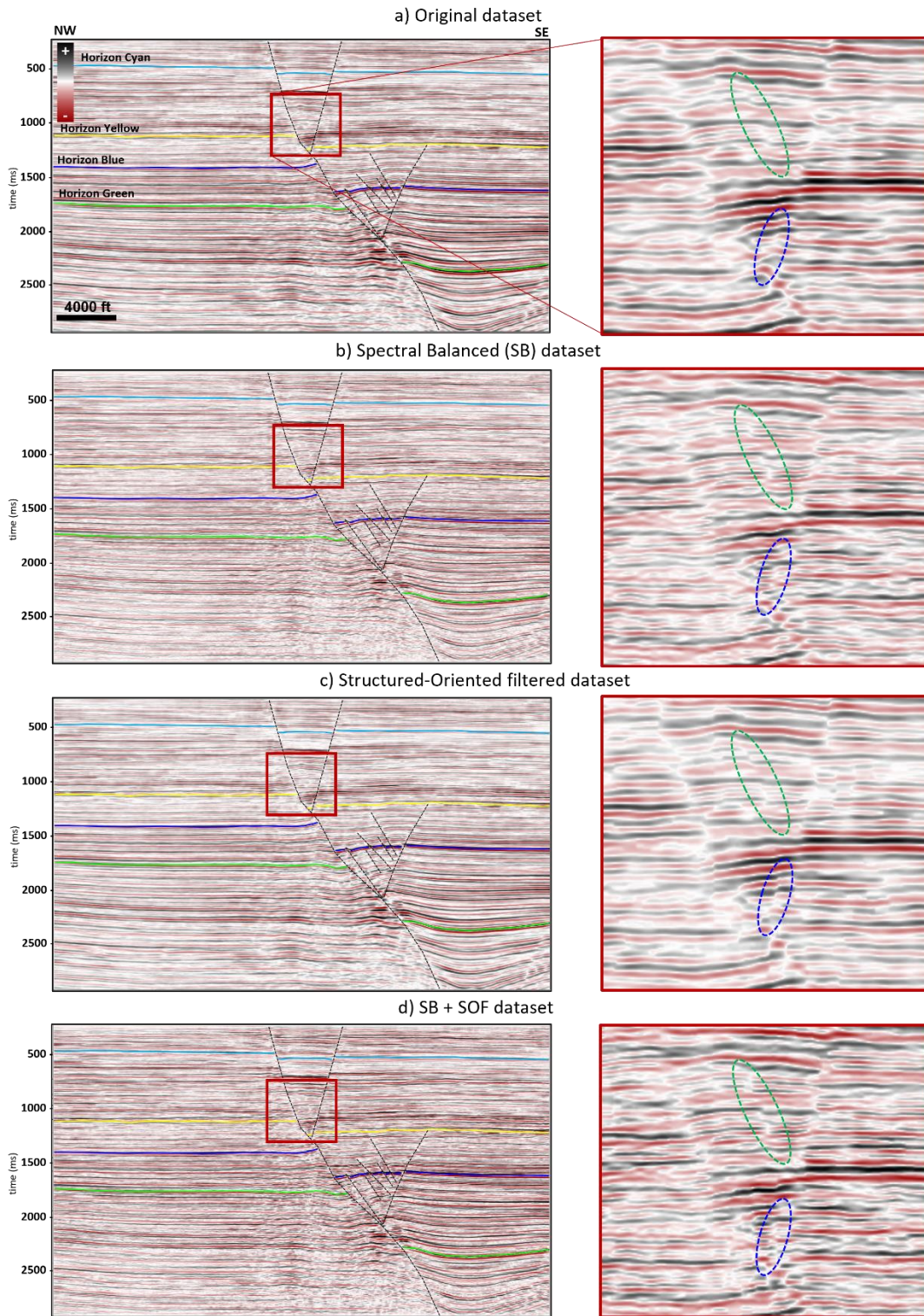
Figure 9. *Seismic inline with interpretation through the different volumes used in this study: a) original dataset, b) spectrally balanced dataset, c) structure-oriented filtered dataset, and d) spectrally balanced and structure-oriented filtered dataset. The location of this crossline is referenced in Figure 1.*

Figure 10 displays the seismic Crossline 2180, and they attempt to show how spectral balance, structure-oriented filter, and spectral balance plus structure-oriented filter modify the original dataset. Since crosslines are perpendicular to the seam of the two cubes, they are useful to observe the impact of the conditioning methods on the mismatch of frequencies and amplitudes.

Figure 10-a displays the original dataset, and we can easily highlight where the seam between the two legacy surveys occurs, especially in the shallowest part. Over this section, we can point out that the amplitudes are brighter in the NE area. Additionally, the change of frequencies is observable in the change of thickness of the seismic events.

In Figure 10-b, we can observe how spectral balance modifies the dataset. There is an improvement in the amplitude distribution, and we can see that the amplitude contrast is subtler now. Additionally, as we saw in Figure 9-b, the frequency of the reflectors is higher and balanced, thus helping to reduce the contrast on both sides of the seam.

The effect of the structure-oriented filter on the dataset is visible in Figure 10-c. We can see that the frequencies and amplitude distribution are not changed when they are compared to the original dataset in Figure 10-a. This is an expected result since SOF is not a method applied to address the problem of the mismatch between the two legacy cubes but is applied to improve the edges visualization.

The result of applying spectral balancing followed by SOF can be seen in Figure 10-d. As we can observe, we obtained the same results regarding amplitudes and frequency distribution as we got when we only applied spectral balance, but additionally, we have an improvement in the faults visualization and stratigraphic edges. As a result of applying spectral balance and SOF, we can also observe an artifact occurring, especially in the deepest seismic events. We can observe

that said reflections lost their smooth continuity and have a "blocky" appearance. This artifact is known as the stair-step effect (Lin and Marfurt, 2017).
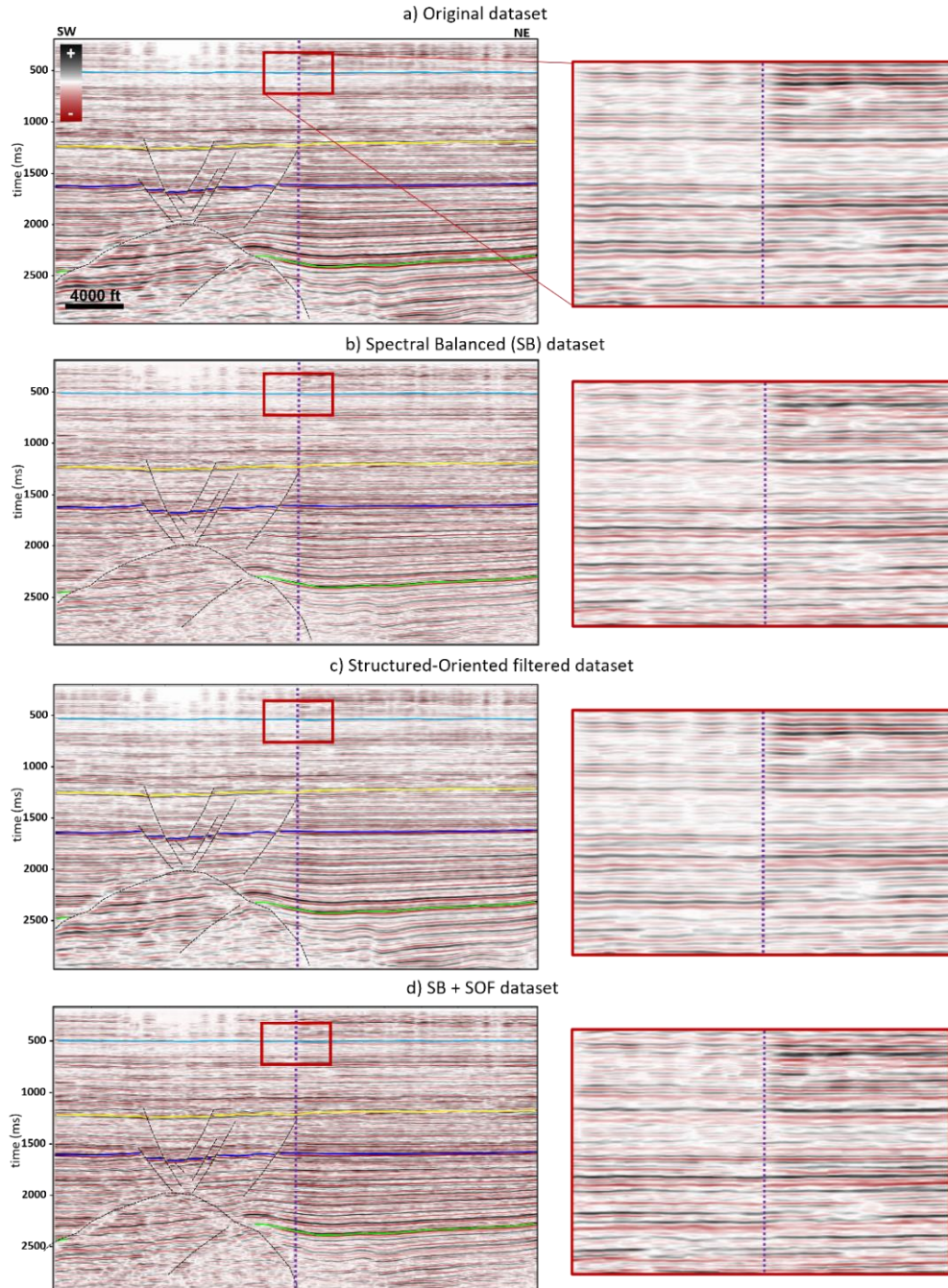
Figure 10. *Seismic crossline with interpretation through the different volumes used in this study: a) original dataset, b) spectrally balanced dataset, c) structure-oriented filtered dataset, and d) spectrally balanced and structure-oriented filtered dataset. The location of this crossline is referenced in Figure 1.*

We ran the attributes described in Table 2 and created horizon slices over Horizon Blue using the abovementioned volumes as input. Appendix A further explains the theory behind the attributes analyzed in this project.

Results on single trace attributes

Envelope

This attribute is sensitive to changes in acoustic impedance. We observe in Figure 11 that after applying spectral balance, the amplitudes were reduced from a maximum value of 35,000 to a maximum value of 27,500, meaning a 22% of reduction. Even though we still have an amplitude contrast at both sides of the seam, we observe that the distribution of amplitudes is more homogeneous in that area. These are all expected results according to the spectral balance theory and the frequency spectrum analysis of the datasets. Despite this attribute not being ideal for analyzing structures, we see that both spectral balancing and structure-oriented filtering modify the imaging of the main fault and, in general, enhance its visualization. Additionally, the green circle in Figure 11-b and Figure 11-d points out that after spectral balancing, there is a change in the imaging of the main fault system, showing minor structures next to the Clemente-Tomas fault that were not visible before.

.

Figure 11. *Amplitude extraction over Horizon Blue on envelope cube calculated in a) the original dataset, b) the spectrally balanced dataset, c) the structure-oriented filtered dataset, and d) both spectral balanced and structure-oriented filtered dataset. Black arrows point to faults observed in this horizon slice. The orange arrow denotes the sharp amplitude contrast at the seam and the yellow arrow indicates the seam between the two surveys. The red dashed circle indicates an improvement in fault visualization after spectral balancing.*

Instantaneous frequency

This attribute is helpful in identifying attenuation and thin-bed tuning. Figure 12 shows that frequency values increased after spectral balancing, and the color bar histogram shows a broad frequency spectrum. Figure 12-b and Figure 12-d display a frequency range from 10 Hz to 50 Hz,

while the original dataset ranges from 15 Hz to 40 Hz. Both the original and the structure-oriented

filtering display a sharp contrast at the seam area. In Figure 12-a and Figure 12-c, we can observe

that frequencies at the left side of the seam are in the range of green-yellow colors, which means

a bandwidth between 30 Hz and 35 Hz, and at the right side of the seam, they are on the range of

the blue-green colors, which means a bandwidth between 25 Hz and 35 Hz. Such difference in

values at both sides of the seam denotes a frequency contrast unrelated to a geological event since,

as we can observe, it is perfectly aligned with the union of the original cubes. Even though the

differences between Figure 12-b and Figure 12-d are subtle, the results of combining two

conditioning methods seem to help homogenize and equalize the frequency values across the seam.

Figure 12. *Amplitude extraction over Horizon Blue on Instantaneous Frequency cube calculated in a) the original dataset, b) the spectrally balanced dataset, c) the structure-oriented filtered dataset, and d) both spectral balanced and structure-oriented filtered dataset. Black arrows point to faults observed in this horizon slice. The orange arrow denotes the sharp amplitude contrast at the seam, and the yellow arrow indicates the seam between the two surveys.*

Results on geometric attributes

Sobel filter similarity

This attribute is helpful for stratigraphic edges and faults visualization. Figure 13 shows that this attribute is not sensitive to the amplitude contrast at both sides of the seam, and there is no visible difference in amplitudes across the union of the cubes. This attribute is a great example

of how spectral balancing and structure-oriented filtering improve the visualization of geometries over the horizon. Figure 13-b depicts some features that are attributed to footprint noise, highlighted in the red dashed lines circles, that are not as visible in the original dataset. This might be an undesired result of spectral balancing. However, improvements in the visualization of faults are highlighted in a green dashed line circle. Interestingly, the application of spectral balancing displays a set of small faults parallel to the Clemente-Tomas Fault (Figure 13-b) that SOF cannot display when applied without previously balancing the data (Figure 13-c). This leads to at least two possible scenarios the interpreter must carefully evaluate to accurately interpret the geology. The first possible scenario is that spectral balancing highlights noise and creates fault-looking artifacts, and the second scenario is that SOF is not able to resolve these small features. Both cases require the integration of geophysical and geological criteria to conclude the most accurate interpretation.
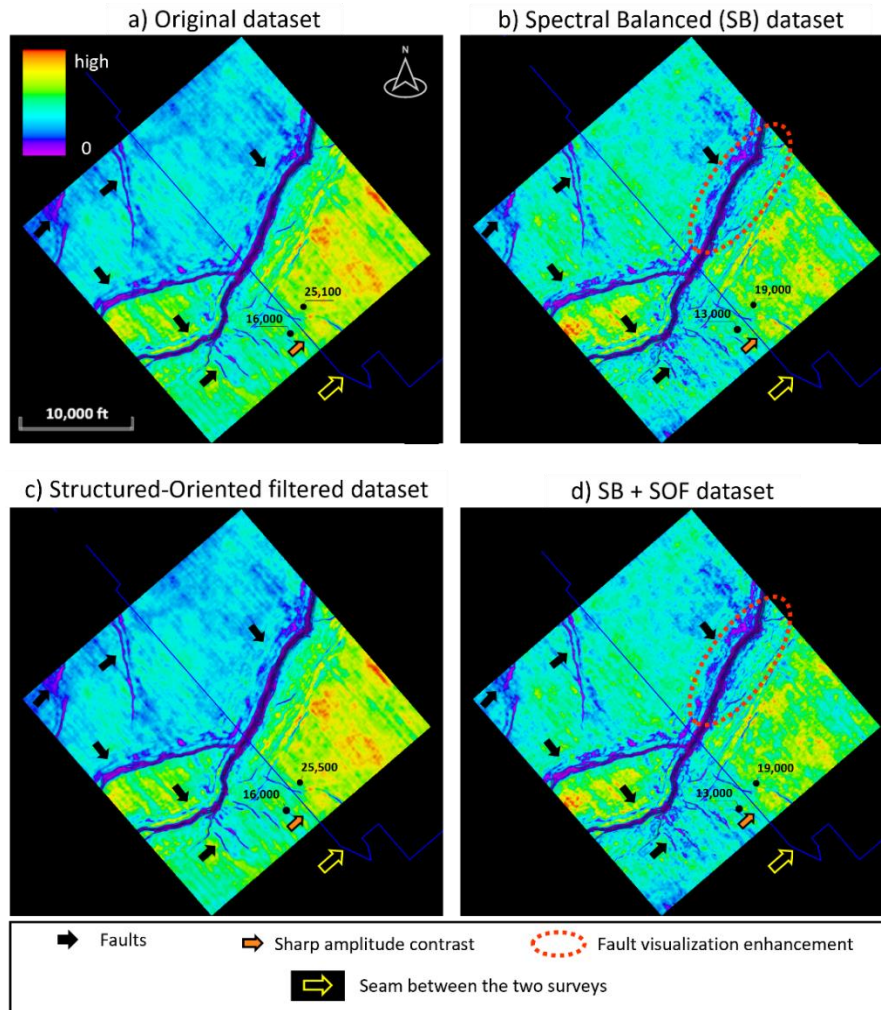
Figure 13. *Amplitude extraction over Horizon Blue on Sobel Filter cube calculated in a) the original dataset, b) the spectrally balanced dataset, c) the structure-oriented filtered dataset, and d) both spectral balanced and structure-oriented filtered dataset. The yellow arrow indicates the seam between the two surveys. Black arrows point to faults observed in this horizon slice. The green circles show fault visualization enhancement after spectral balancing, end the red circles indicate footprint noise exacerbated after data conditioning.*

Total energy

This geometric attribute effectively distinguishes low-energy chaotic reflectors from seismic responses exhibiting higher energy. Its application over the Horizon Blue resulted very efficiently in depicting the sharp amplitude contrast on both sides of the seam. However, this

attribute appears insensitive to the effects of seismic conditioning methods, as evidenced by the similarity in the four maps shown in Figure 14, with just subtle differences. These findings show a very limited contribution for the purpose of homogenizing the distribution of amplitudes of the merged cube. The most pronounced impact is observed in Figure 14-b and Figure 14-d, where spectral balancing is applied, resulting in a reduction of amplitude contrast between the footwall and hanging wall compared to the original dataset.
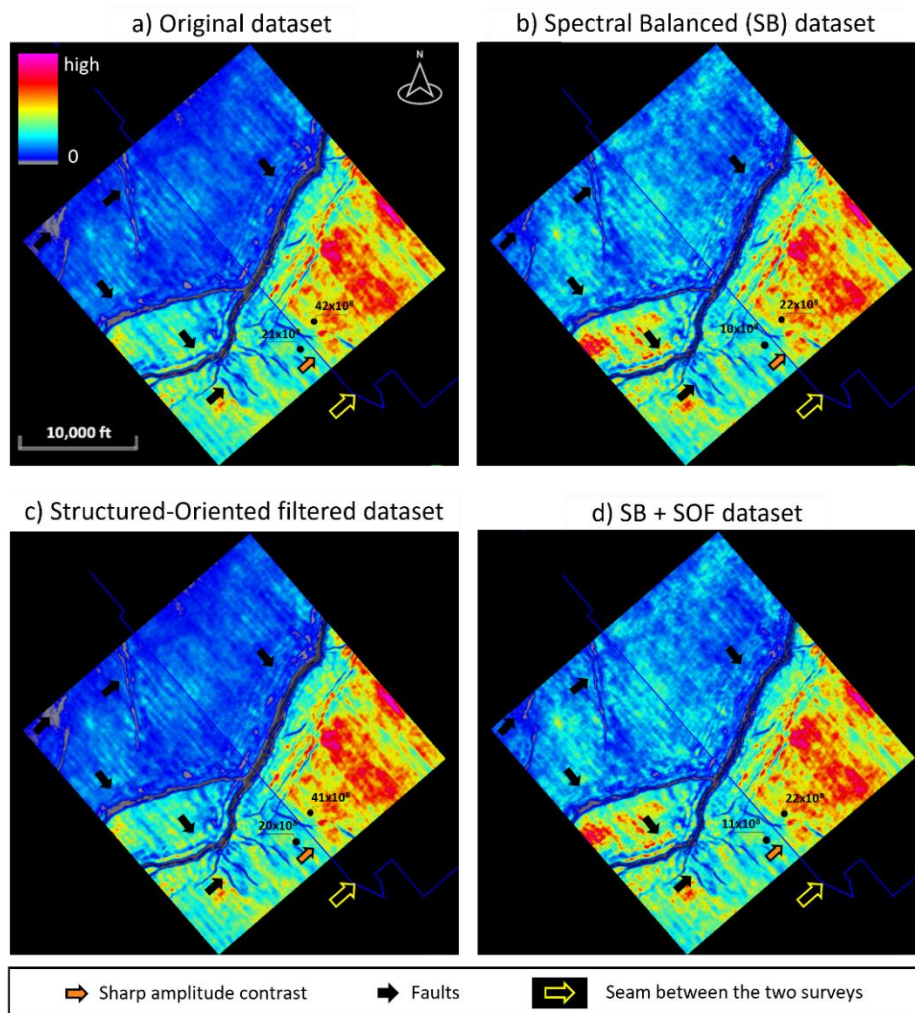
Figure 14. Amplitude extraction over Horizon Blue on total energy cube calculated in a) the original dataset, b) the spectrally balanced dataset, c) the structure-oriented filtered dataset, and d) both spectral balanced and structure-oriented filtered dataset. Black arrows point to faults observed in this horizon slice. The orange arrow denotes the sharp amplitude contrast at the seam, and the yellow arrow indicates the seam between the two surveys.

Results on spectral attributes

Peak magnitude

This attribute computes the maximum magnitude value within the average spectral frequency in a voxel, and it is a strong hydrocarbon indicator. Similar to what we observed in the results of envelope, Figure 15 depicts that the peak magnitude calculated on the original dataset displays a sharp contrast in the seam area. In Figure 15-a, the value of the attribute on the left side of the seam is around 55,000, while on the right side, it is around 100,000, meaning a 45% difference. This high contrast, which we can tell has no geological meaning and aligns perfectly to the seam, is attenuated after applying spectral balance, reducing the difference to a 30% of the values, as shown in Figure 15-b and Figure 15-d. These maps show that spectral balancing homogenizes the values at both sides of the seam, thus reducing, but not eliminating the sharp contrast.
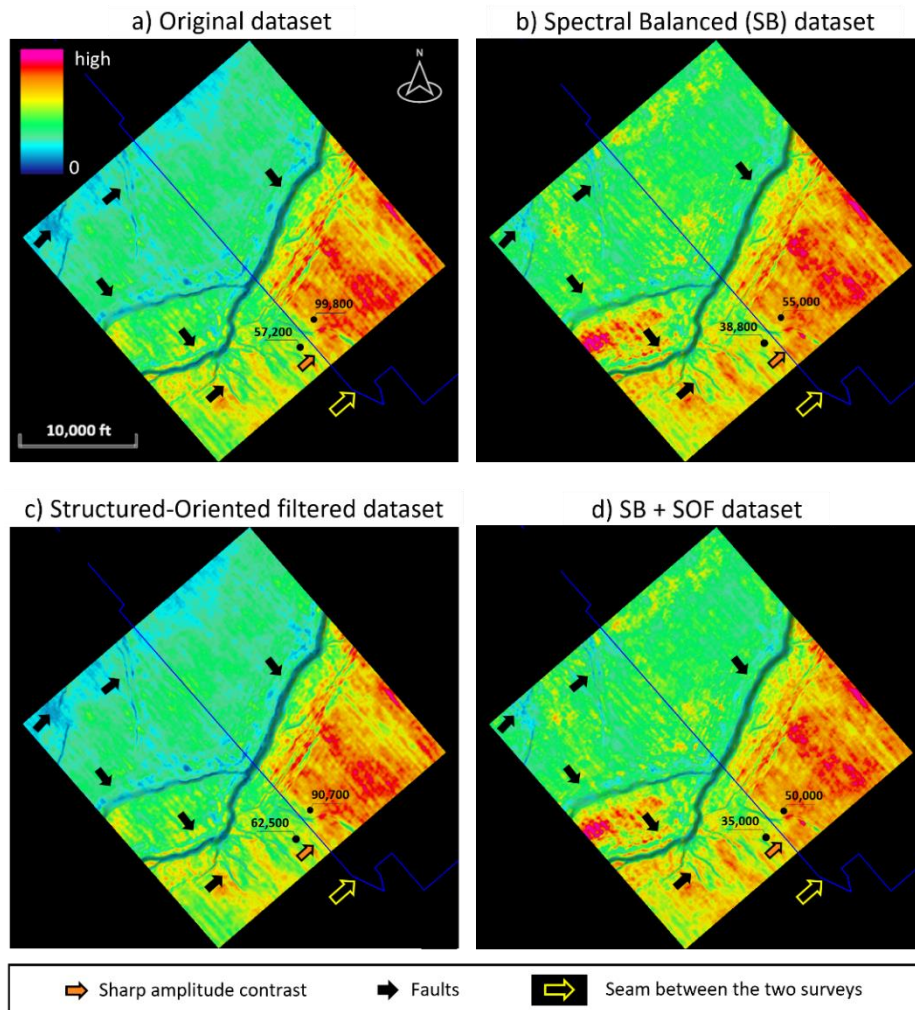
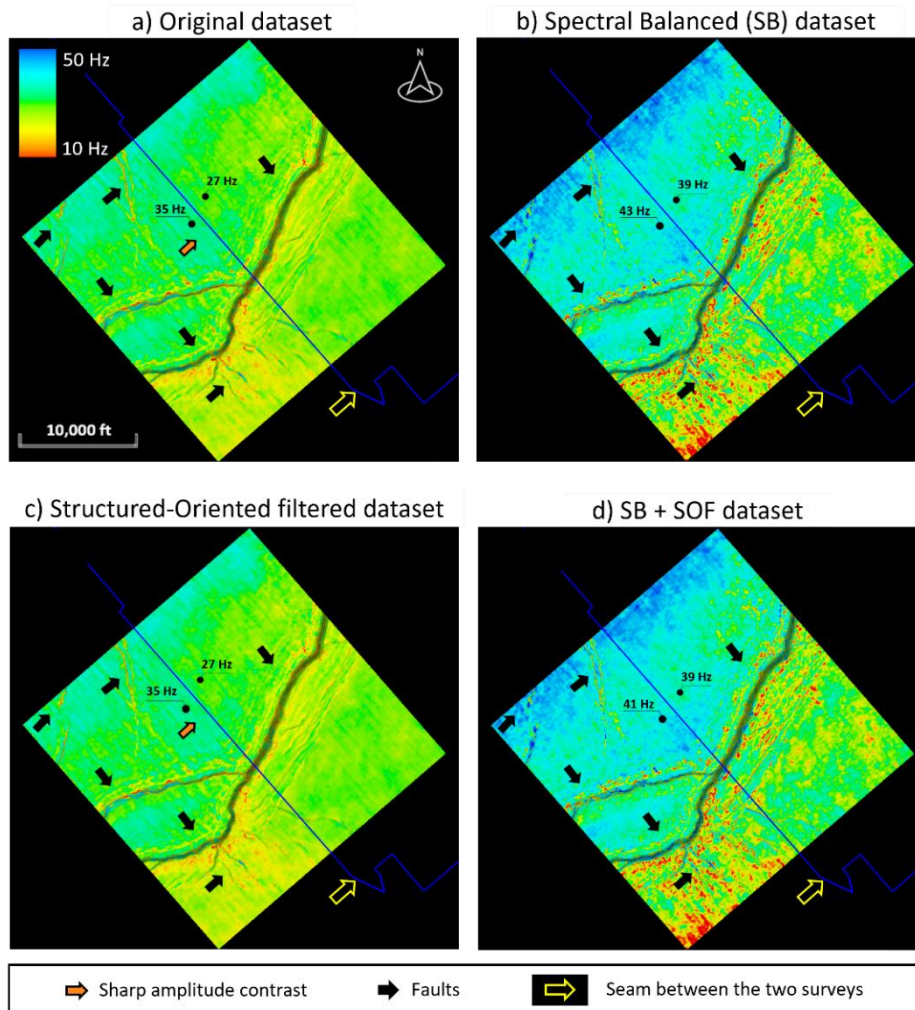*Figure 15*. *Amplitude extraction over Horizon Blue on Peak Magnitude cube calculated in a) the original dataset, b) the spectrally balanced dataset, c) the structure-oriented filtered dataset, and d) both spectral balanced and structure-oriented filtered dataset. The orange arrow denotes the sharp amplitude contrast at the seam, and the yellow arrow indicates the seam between the two surveys.*

Mean frequency

This attribute computes the mean frequency value within the average spectral frequency in a voxel, and it is helpful in detecting thin-bed tuning anomalies. As a general statement, the results we obtained applying this attribute were the most valuable for homogenizing the data across the merged dataset. We can observe in Figure 16-a that on the original dataset, the frequency contrast

is still visible, but the difference between the values at both sides of the seam is not as big as in other attributes. The application of spectral balance in Figure 16-b shows a great reduction in the amplitude contrast, displaying frequencies around the same value at both sides of the seam. Additionally, we can observe how the histogram of the color bar displays a broader frequency spectrum after spectral balancing, ranging from 27 Hz to 40 Hz in the original and SOF datasets and 32 Hz to 52 Hz in the spectrally balanced datasets. This increase in frequency values is an expected result, as we mentioned in the theory, but also, what is remarkably valuable for this project is that the distribution of the values is such that the sharp contrast due to the merging of two different cubes is notably reduced, as we can note in Figure 16-b and Figure 16-d.
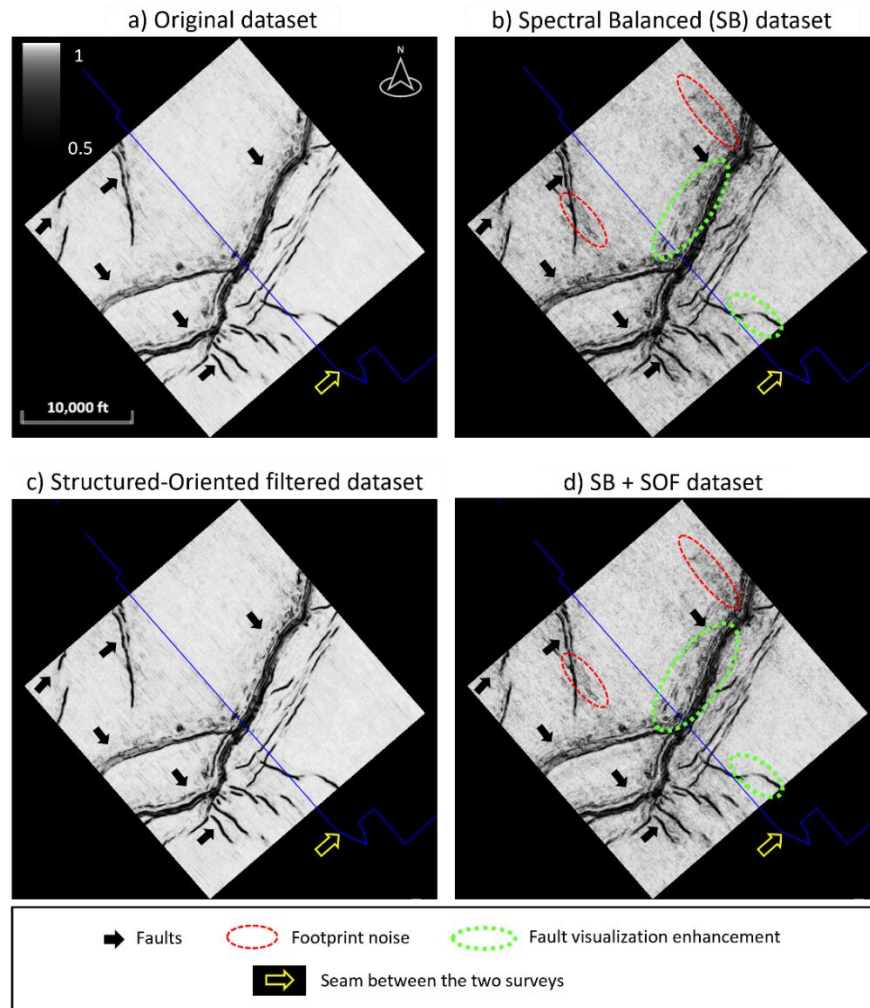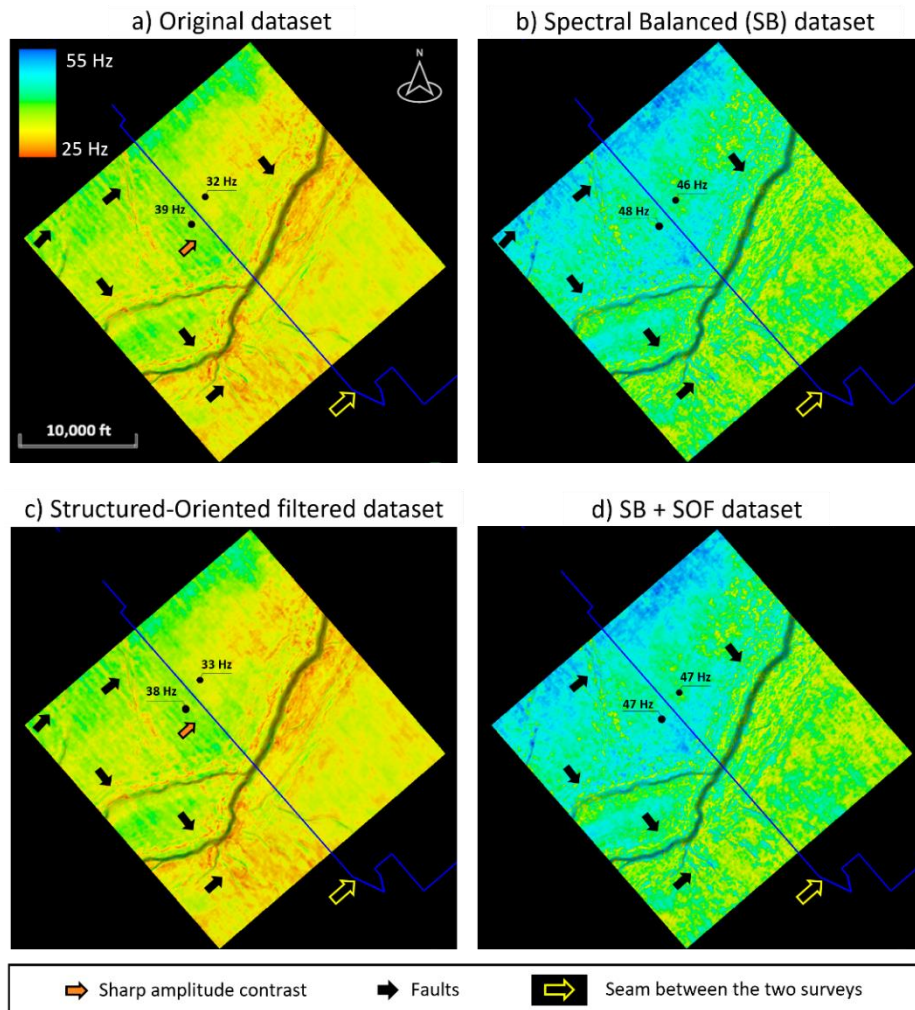
Figure 16. *Amplitude extraction over Horizon Blue on Mean Frequency cube calculated in a) the original dataset, b) the spectrally balanced dataset, c) the structure-oriented filtered dataset, and d) both spectral balanced and structure-oriented filtered dataset. The orange arrow denotes the sharp amplitude contrast at the seam, and the yellow arrow indicates the seam between the two surveys.*

DISCUSSION

The primary aim of this project is to enhance the quality of a merged dataset using various seismic data conditioning workflows. A key challenge within this dataset is the significant disparity in amplitude and frequency values resulting from an inaccurate merging of two legacy

cubes, compounded by a prevalence of low-frequency content and footprint noise along the NE-SW direction. Given these situations, the interpreter can apply different post-migration seismic data conditioning methods. In this case, we evaluate the impact of applying a trace-by-trace spectral balance to overcome the mismatch of values and homogenize the dataset across the seam between the two cubes. Additionally, we followed spectral balancing with structure-oriented filtering to sharpen the features that were revealed in the previous step. To assess the impact of each process, we first applied each method independently over the original dataset and then in combination. The application of trace-by-trace spectral balancing may be aggressive for the relative amplitudes (Marfurt, 2018), harming them in such a way that the data might require an exhaustive data control for an advanced evaluation of AVO or impedance inversion. However, since our objective is to reduce the contrast in the seam of two different cubes to have a more accurate geologic interpretation, we decided that this might be the best approach to overcome this issue. This initial step aims not only for a more uniform distribution of frequencies and amplitudes throughout the cube but also anticipates a finer delineation of stratigraphic edges and faults, leading to improved resolution. To go further in the improvement of the data quality, we applied the well-known technique in the industry, structure-oriented filtering (Hocker and Fehmers, 2002), to highlight faults and stratigraphic edges, thus obtaining a more complete and detailed geologic interpretation.

The application of filters and algorithms to improve the data quality is not a mere routine task in which the interpreter uses the same workflow for every seismic dataset. Especially when frequencies are modified, the interpreter must use all the geophysical and geological criteria applicable to solve a problem. Determining whether the features revealed with the spectral balancing hold geological significance is crucial. To do so, we generate seismic sections by cutting

perpendicularly through these features and analyzing how the processes altered the original data. The analysis includes the visualization and comparison of results before and after seismic data conditioning on the merge, discussing the impact on the geologic and seismic interpretation of the data, focusing especially on the sharp contrast of amplitude and frequency values observed at the seam, and the visualization of faults.

Amplitude-based attributes aspects

The amplitude-based attributes have not completely homogenized the values across the seam in the instantaneous and spectral results. This result, observed in envelope and peak magnitude attributes, might be the consequence of applying a trace-by-trace spectral balance. In our implementation, spectral balancing preserves the relative amplitude of each trace in a statistically reasonable manner (Marfurt, 2018), effectively diminishing the discrepancy in frequencies across the surveys. However, it struggles to fully mitigate the amplitude contrast. To address the amplitude problem, a further step can be followed, which is the application of automatic gain control (AGC).

Although in this project we are applying it to migrated data, AGC is a well-known method that is applied during the processing stage. As spectral balancing, this is also a trace-by-trace algorithm, and it attempts to recover the amplitude of the signal that has been dissipating during the propagation of the wave through different mediums (Dondurur, 2018). AGC can severely modify the natural reflection of a seismic reflector, making it a very aggressive process for seismic data and must be used carefully. Its application may remove relative amplitudes, avoiding the correct interpretation of the depositional environment or hiding bright spots. We ran AGC using different window lengths to investigate how this algorithm modifies the merged data and if it is possible to homogenize amplitudes at both sides of the seam. The window length or AGC operator

length (Dondurur, 2018) is critical since it determines the scale factor used to homogenize the amplitudes along the trace. In Figure 17, we can see a seismic crossline through the cube, displaying the union between the legacy surveys, represented by the grey dashed vertical line. Figure 17-a displays how the seismic looks in the original dataset, Figure 17-b spectrally balanced and structure-oriented filtered dataset, Figure 17-c spectrally balanced and structure-oriented filtered dataset applying AGC with a 0.5-second operator length (long window), and Figure 17-d spectrally balanced and structure-oriented filtered dataset applying AGC with a 0.05-second operator length (short window).

As we expected, the amplitudes look equalized in the entire survey and it is evident that we do not observe the sharp amplitude contrast on both sides of the seam after applying AGC. However, to analyze how the different AGC operators work in the data, we need to identify the changes this algorithm has made. We observe that there is a substantial difference between Figure 17-c and Figure 17-d. One method to demonstrate this difference is by examining the seismic response of Horizon Blue. In both the original and spectrally balanced and SOF datasets, Horizon Blue, owing to its strong reflectivity, serves as a prominent horizon that is easily discernible throughout the entire volume. However, upon applying AGC, we observe a gradual loss of its inherent reflectivity, with its prominence diminishing each time we reduce the operator length. The interpreter must be very careful with using this tool and selecting the operator's length. If the objective is to perform an amplitude analysis, then this algorithm should be applied always with well control and ideally using a long window, such as 0.5 seconds. However, we do not recommend this practice for an amplitude analysis since essential changes in the amplitude of the seismic events can be severely modified, as we can see with the bright spot highlighted in the green circle in Figure 17. Again, we can witness how the bright spot is lost as we diminish the AGC operator.

On the other hand, if the intention is to interpret geometries, such as sequential stratigraphy geometries, pinch-outs, or chaotic low-amplitude reflections, then a short window can aid the visualization of them. We can observe in Figure 17-d how the low reflectivity horizons highlighted in the turquoise circle are better visualized using a short window length in the application of AGC.
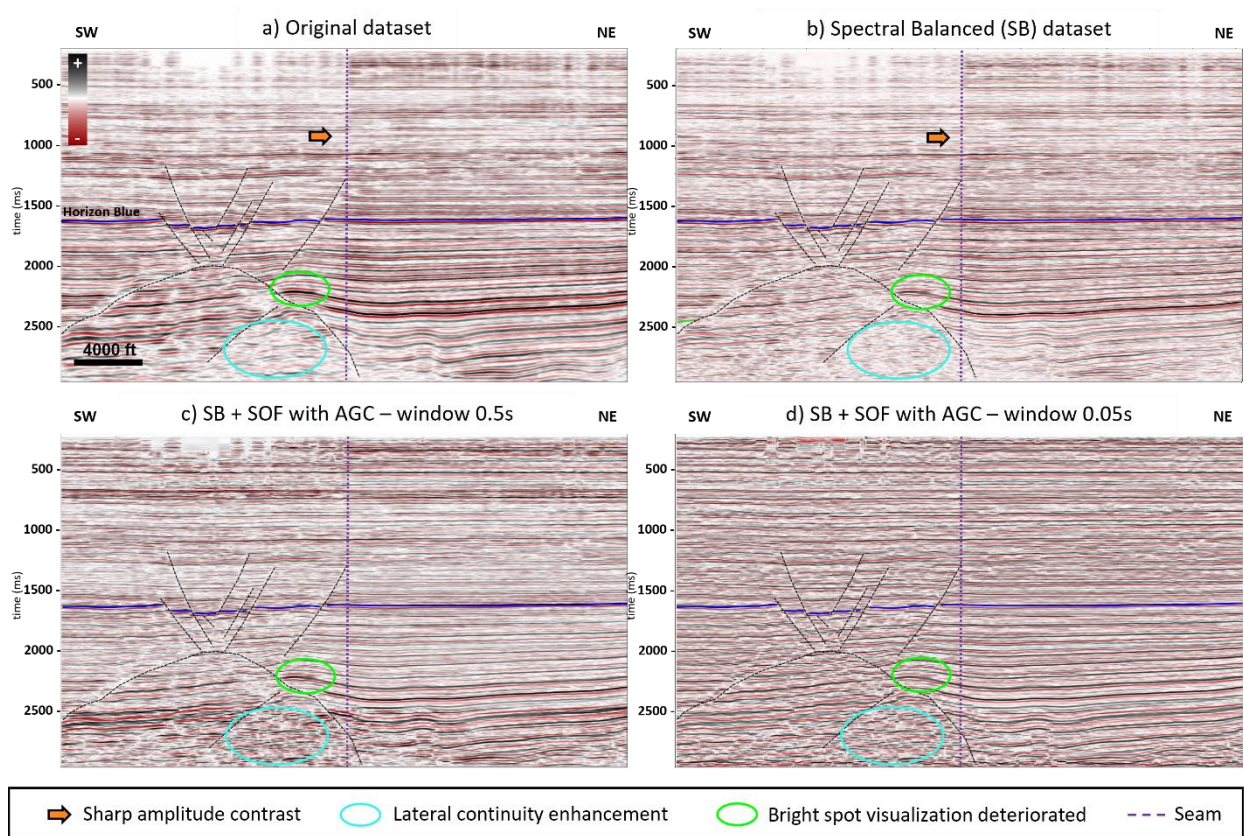
Figure 17. *Seismic crossline through a) original dataset, b) spectrally balanced and structure-oriented filtered dataset, c) spectrally balanced and structure-oriented filtered dataset applying AGC with a 0.5-second operator length (long window), and d) spectrally balanced and structure-oriented filtered dataset applying AGC with a 0.05-second operator length (short window).*

Geometric attributes aspects

Geometric attributes provided insightful results that may change the geologic interpretation after applying spectral balancing and structure-oriented filtering, especially when we look at Sobel

filter (semblance). We can observe in Figure 13 that there are remarkable differences between the results obtained by applying each method independently. Spectral Balancing displays some artifacts parallel to the main structure. We examined the seismic in the inline direction (perpendicular to the Clemente-Tomas fault) to determine if those artifacts parallel to the fault are part of the main structure or artifacts due to the strong presence of noise.

In Figure 18, we observe that these features correspond to a deformation over the horizon close to the main fault in the footwall block. These subtle flexures, indicated with yellow arrows, were not highlighted by the application of a structure-oriented filter by itself but were revealed with the application of spectral balance. This is an expected effect of this algorithm since by relocating usable data frequencies to their ideal position; we were able to resolve small-scale faults that provide a complete understanding of the geology.

Given the context of a low-quality seismic resolution, it becomes necessary to quantify how 'small' these newly revealed features are. This area is conformed by interlay sand and shale without the presence of other lithology that generates a velocity anomaly, such as a salt dome or an igneous body. If we consider average velocities for sand and assume a P-wave velocity of 6,500 ft/s at the depth of Horizon Blue, then we obtain that the thickness of the reflector (λ) is about 230 ft (Figure 18-a). As a reference, the height of the Sarkeys Energy Center building at the University of Oklahoma campus is 210 ft, so the estimated thickness of this reflector is about the same height. This value indicates that the minimum thickness -or tuning thickness (Widess, 1973)- that can be detected at that depth in the original volume is $\lambda/4 \approx 60$ ft, a package of more than 5 stories of the Sarkeys building. After spectral balancing, as shown in Figure 18-b, the thick reflector now has more definition, and we can see more detail on it. Repeating the same reasoning used to calculate the thickness of the reflector in the original dataset, we calculate the thickness of the revealed

reflectors after seismic data conditioning and obtained that now instead of looking at a 230 ft reflector, we observe a 120 ft horizon, with an estimated tuning thicknesses around 30 ft (about three stories of the Sarkeys building). In light of these results, then the small-scale features revealed after spectral balancing observed through the Sobel filter are no bigger than 250 ft on the horizontal and 30 ft on the vertical scale.
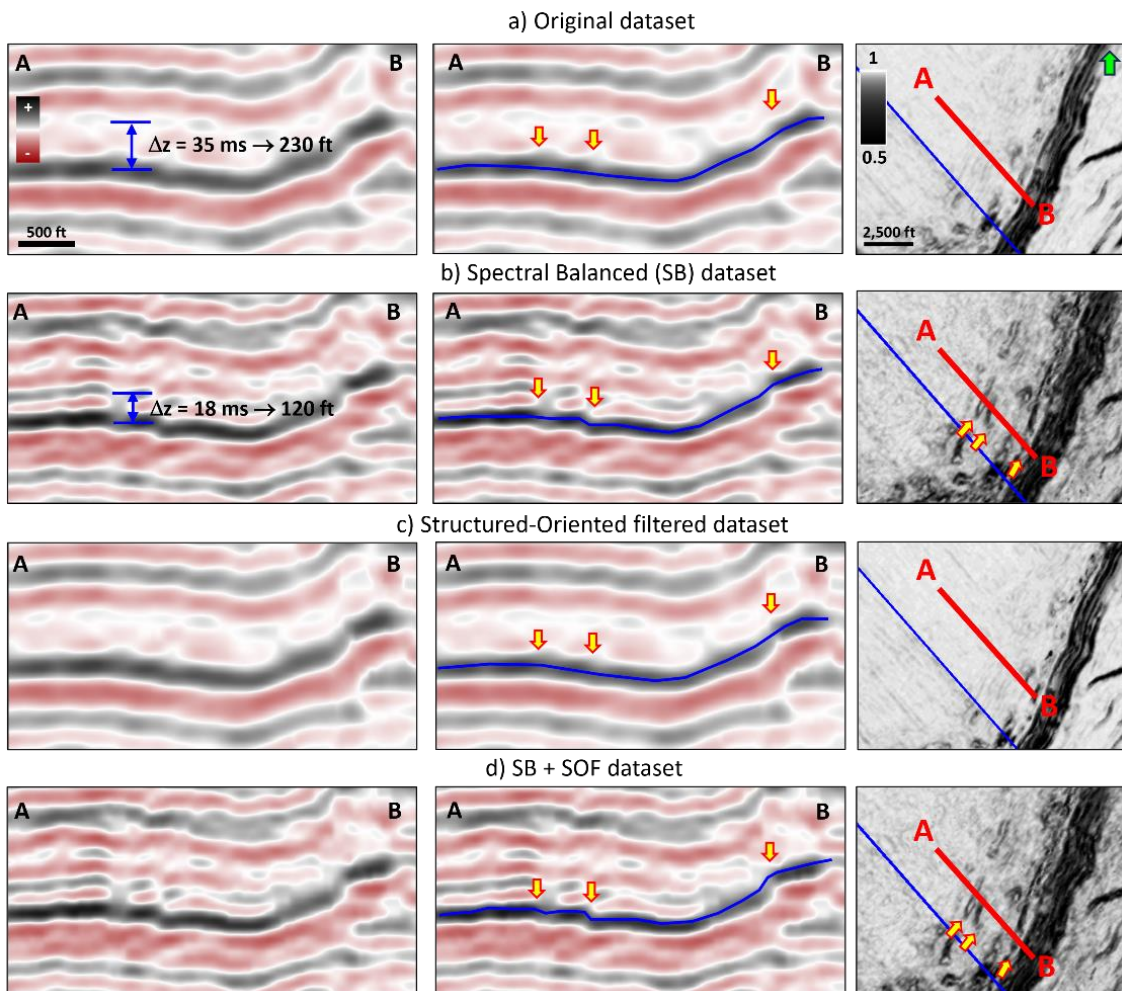
Figure 18. *Detailed seismic section perpendicular to the features revealed after spectral balancing without interpretation in the left column and interpreted in the center column, correlated with the Sobel filter attribute at the right column in the a) original dataset, b) spectrally balanced dataset, c) in the structural-oriented filtered dataset, and d) in the spectrally balanced and structure-oriented filtered dataset. The yellow arrows indicate where these subtle events occur.*

Another remarkable difference observed before and after seismic data conditioning on Sobel filter is visible at the southeast of the Clemente-Tomas fault, in the hanging wall block. There, we can see an increase in noise in Figure 13-b and Figure 13-d. With the objective of understanding if this noise is a product of exacerbation of footprint noise due to the application of spectral balance, we created detailed seismic sections in that area to make a refined interpretation. Figure 19 displays in detail this area on the different maps and cross sections. Given the magnitude of this major fault trend in offshore Texas, it is reasonable to anticipate a pronounced level of deformation and faulting. Upon observation, we note that small-scale deformation remains unresolved solely through the application of structure-oriented filtering. However, when combined with spectral balancing, we discern that the noise apparent post-conditioning originates from minor faults within this block, generating rugosities over Horizon Blue. This scenario highlights a case where the noise observed stems from the geological context and sediment deformation rather than acquisition or processing artifacts.
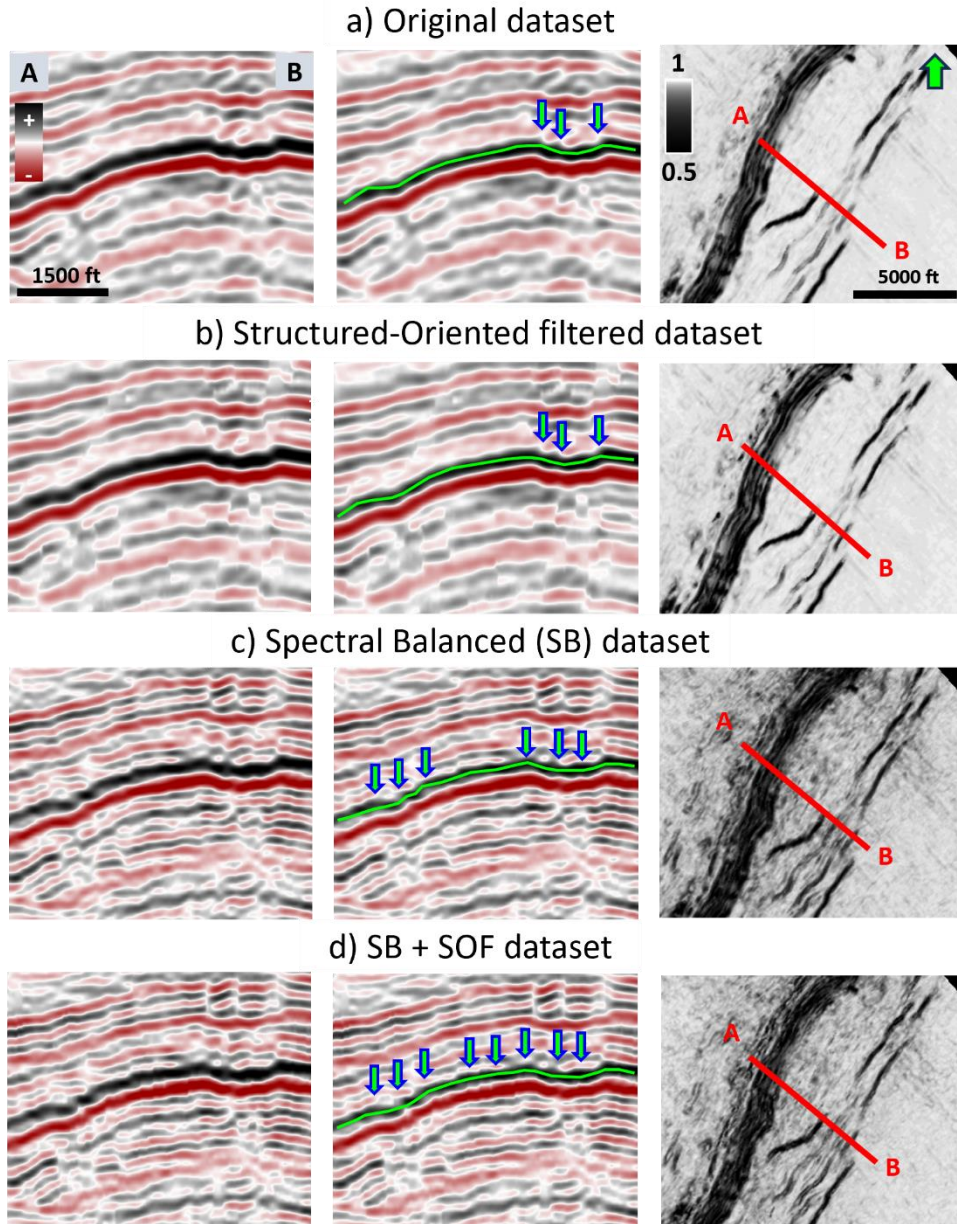
Figure 19. *Detailed seismic section perpendicular to the features revealed after spectral balancing without interpretation in the left column and interpreted in the center column, correlated with the Sobel filter attribute at the right column in the a) original dataset, b) spectrally balanced dataset, c) in the structural-oriented filtered dataset, and d) in the spectrally balanced and structure-oriented filtered dataset. The arrows indicate the discontinuities highlighted over the horizon in each conditioning workflow. Notice how the horizon displays more' rugosities' in the SB + SOF dataset compared to the other cases.*

Frequency-based attributes aspects

The application of spectral balancing significantly improved the frequency distribution across the volume. Both Figure 12-d and Figure 16-d display how spectral balance effectively reduced the dependence of the seam for a frequency analysis. This means that after applying spectral balancing, the relative contrasts of the frequencies are no longer conditioned by the union of the legacy surveys. The implications of this outcome could significantly influence geological interpretation, potentially leading to substantial misinterpretation of the tuning phenomena prior to implementing spectral balancing in our dataset.

Integrated analysis

The previous section showed the impact of each seismic data conditioning process when we are visualizing seismic attributes. In a higher or lower grade, we observed how the data changed after applying each of the techniques described above. To give an additional assessment, Figure 20 displays the corender of three different attributes in a time slice at 932 milliseconds. It shows peak frequency, peak magnitude (without the application of AGC), and Sobel filter. Note the different color bars used to display three attributes simultaneously. We chose a conventional frequency color bar for frequency, and monochromatic colors for peak magnitude, as well as a Sobel filter, with opacities that help us highlight what we are interested in seeing from the data. In this case, giving full opacity to high peak magnitude values allows us to see those areas where we have lithologies with both high frequency and high amplitude values and hides those areas where the amplitudes are low. Similarly, opacity in Sobel filter serves as a highlighter of edges while mutes areas where the attribute doesn't show discontinuities.

Figure 20. *Corendered time slice at 932 ms displaying peak frequency – peak magnitude – Sobel filter. in a) the original dataset, b) the spectrally balanced dataset, c) the structure-oriented filtered dataset, and d) both spectral balanced and structure-oriented filtered dataset. Arrows in different colors point to several features modified after applying seismic data conditioning methods.*

Figure 20 provides a comprehensive assessment of how conditioning processes impact the data, enabling us to gauge the effectiveness of these steps in enhancing stratigraphic features and fault visualization within a low-quality dataset. We offer interpretations to emphasize the most

notable observations indicated by arrows in different colors. Arrows in yellow, blue, and red indicate the presence of the sharp amplitude contrast, faults, and stratigraphic edges, respectively, while the yellow dashed line circles show the footprint noise. Figure 20-a and Figure 20-c allow us to observe that there is a sharp contrast across the seam -indicated by the yellow arrows- that does not represent a response of the physical properties of the rock to a geological change. Supported by the previous analysis discussed in the results, this frequency change is attributed to the mismatch of frequencies of the merged volume. Figure 20-b and Figure 20-d, on the other hand, demonstrate a more uniform frequency distribution in the seam area, aligning with our anticipated outcome following the discussion of frequency-based attributes aspects.

However, despite these insights, this particular time slice reveals an interesting feature. The red arrows clearly indicate a stratigraphic edge, likely the boundary of a channel. To better understand this stratigraphic feature, we examine it in more detail in Figure 21.
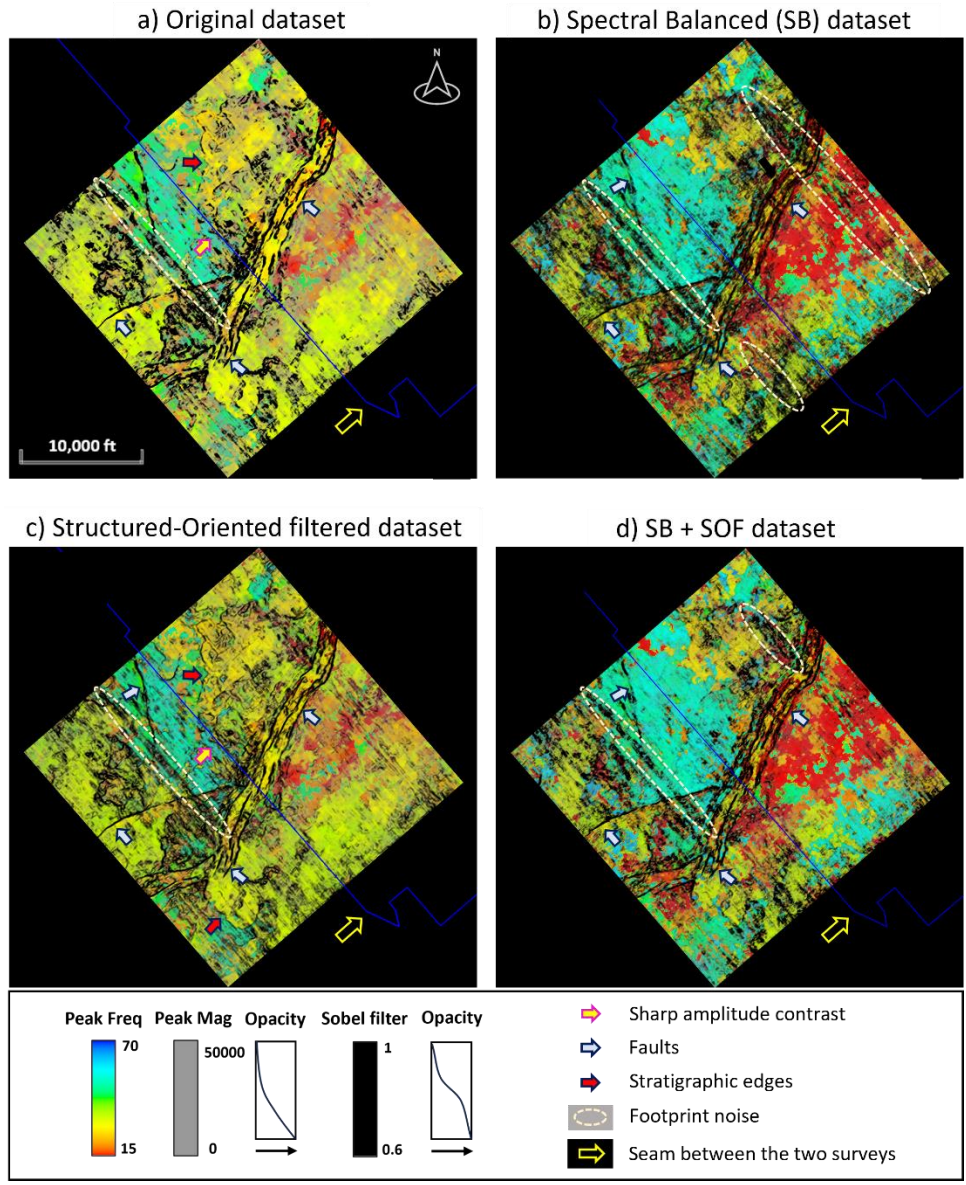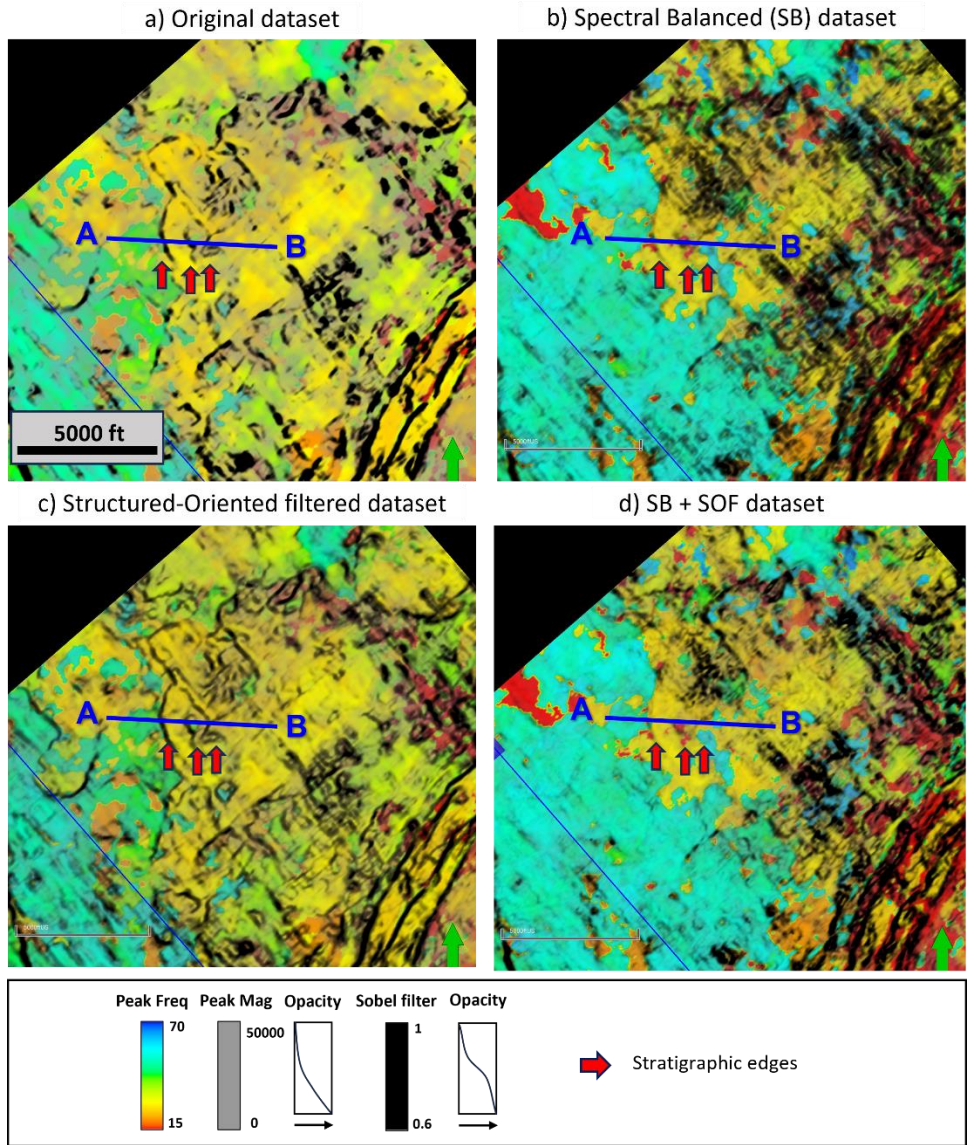
Figure 21. *Zoomed area on stratigraphic edge displaying a corendered time slice at 932 ms displaying peak frequency – peak magnitude – Sobel filter. in a) the original dataset, b) the spectrally balanced dataset, c) the structure-oriented filtered dataset, and d) both spectral balanced and structure-oriented filtered dataset. The arrows indicate the harmed stratigraphic edges, correlating with Figure 22.*
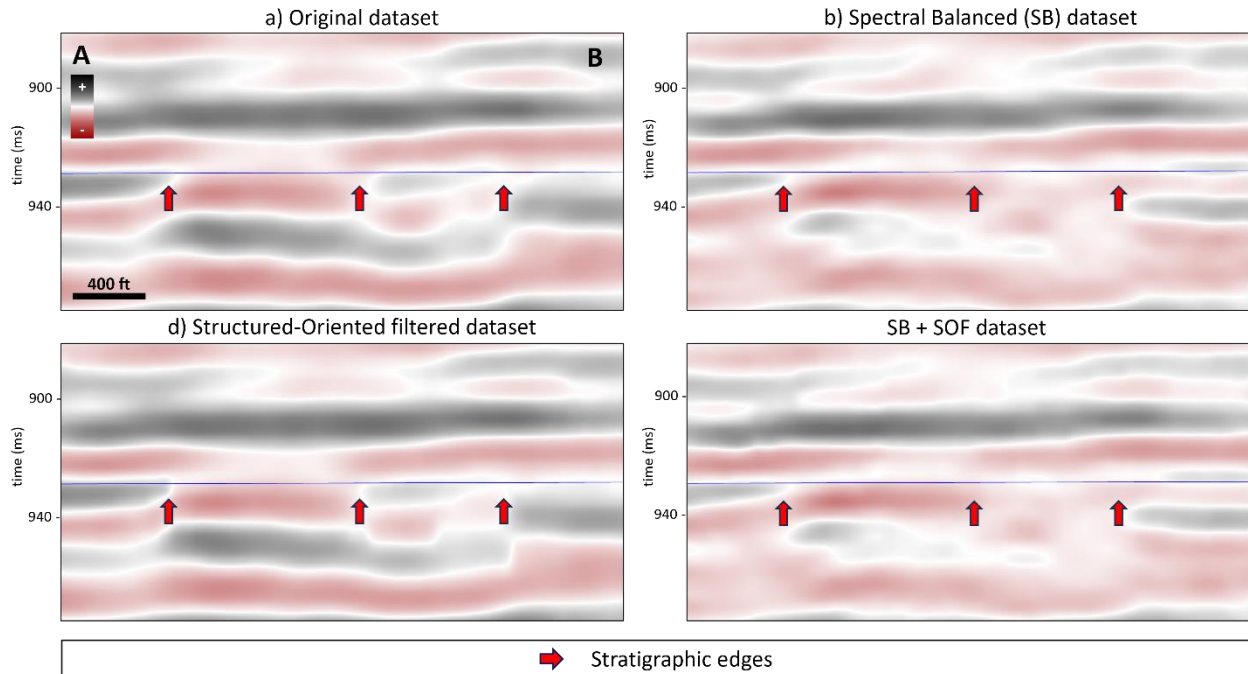
Figure 22. *Detailed seismic section through the harmed stratigraphic edge. The arrows indicate the harmed stratigraphic edges, correlating with Figure 21.*

Figure 21-c illustrates how SOF effectively accentuates the highlighted feature, providing additional detail as anticipated. However, while we expected a significant improvement in visualizing this feature after applying spectral balancing, the results did not meet our expectations. Figure 21 b) and d) and Figure 22 b) and d) demonstrate how spectral balancing adversely affects the data, hindering the visualization of stratigraphic edges. This outcome highlights a potential limitation in using this methodology to enhance data quality.

Previous literature (Marfurt, 2018) has demonstrated that this straightforward methodology employed herein is indeed effective for realigning frequencies to enhance resolution, as confirmed by the frequency spectrum analysis presented in Figure 8 However, our analysis of stratigraphic features reveals a challenge related to tuning frequency (Appendix D). The unbalanced dataset

exhibits a tuning frequency of 20 Hz for the stratigraphic edge. While SOF successfully images this feature without altering the frequency content, spectral balancing broadens and flattens the frequency spectrum, diminishing the delineation of features tuned at this frequency. Consequently, we can highlight faults tuned at different frequencies but struggle to delineate stratigraphic features tuned at 20 Hz.

In addition, we can observe that the footprint is exacerbated after running spectral balance (Figure 21). This is an undesired result on our dataset since the contamination with noise contributes to a poor interpretation of the data, hiding essential features that can change our understanding of the faulting system and/or the depositional environment of the area.

CONCLUSIONS

We assessed the impact of implementing two distinct post-migration seismic data conditioning techniques, spectral balancing and structure-oriented filtering, as well as their combination on a merged dataset. We then analyzed the modifications to the data resulting from these processes. We conducted several attribute analyses to gauge their sensitivity to the challenges inherent in merged datasets and the application of conditioning algorithms. We conclude that:

- The instantaneous, geometric, and spectral attributes used herein were sensitive to the amplitude and frequency dependence produced at the seam of two different surveys.

- After applying spectral balancing:

  o The frequency spectrum was broadened, and the amplitudes were reduced.

  o The magnitude-related attributes still showed a sharp contrast of amplitudes at both seam sides.

- On frequency-related attributes, the contrast at both seam sides was homogenized.

- Footprint noise represented by high frequencies was exacerbated.

- Frequency content is more consistent across the merged cube, allowing a more accurate geological interpretation.

- After applying structured-oriented filtering (SOF):

  - The frequency spectrum is not modified.

  - Faults are sharpened.

  - The footprint noise present in the original dataset is reduced.

- After applying automatic gain control (AGC):

  - The amplitude discrepancy on both sides of the seam is reduced.

  - Relative amplitude differences were harmed using a short operator length.

In particular, for the Matagorda Island dataset, we found that:

- Because the two legacy surveys had different but relatively consistent amplitude and spectra, we could not use an amplitude-friendly survey-consistent correction. Instead, we had to do long vertical window trace-by-trace spectral balancing and amplitude gain control. Implementing trace-by-trace corrections effectively addresses the issues related to frequency and amplitudes. However, their utilization poses risks for impedance inversions.

- Additionally, these methods can also remove lateral variations of interest, such as bright spots and tuning in conventional attribute analysis. In this latter case, we used our understanding of the environment of deposition to verify that we did not compromise the attribute delineation of stratigraphic features of interest.

- Small-scale faults were highlighted after the application of spectral balance.

- Stratigraphic edges tuned at 20 Hz were not improved after applying spectral balancing because of the broadening and flattening of the spectrum frequency. Thus setting a precedent of a pitfall in its application to improve the dataset's quality.

Overall, our examination of applying spectral balancing, structure-oriented filtering, and their combination on a merged seismic dataset revealed significant insights into the impact of such post-migration seismic data conditioning workflows. Spectral balancing broadened the frequency spectrum and homogenized amplitude distribution, facilitating a more consistent geological interpretation. However, we worked with a trace-by-trace algorithm, which can harm relative amplitudes and should always be employed with well control and geological criteria before impedance inversions. In addition, spectral balancing also highlighted footprint noise, an undesired result when we want to enhance the data quality. Meanwhile, structure-oriented filtering sharpened faults and reduced footprint noise but did not alter the frequency spectrum. Notably, our findings caution against relying solely on spectral balancing to enhance stratigraphic features due to decreased tuning frequency, underscoring the need for a nuanced approach to data conditioning. Ultimately, these methodologies offer valuable tools for improving data quality in merged surveys, yet their application requires careful consideration of potential pitfalls and their implications for geological interpretation.

REFERENCES

Ajiboye, O. A. "Structural framework of the Clemente-Tomas and Corsair growth fault systems in the Texas continental shelf margin of the Gulf of Mexico basin." PhD diss., University of Texas at Austin, 2011.

Bally, Albert W., and A. R. Palmer, eds. *Geology of North America—An Overview.* Boulder, CO: Geological Society of America, 1989.

Bose, S., and S. Mitra. "Controls of listric normal fault styles in the northern Gulf of Mexico: Insights from experimental models." *Marine and Petroleum Geology* 35, no. 1 (2012): 41-54.

Bradshaw, B. E., and J. S. Watkins. "Growth-fault evolution in offshore Texas." In *Gulf Coast Association of Geological Societies Transactions*, vol. 44, 1994.

Chopra, S., and K. J. Marfurt. "Spectral decomposition and spectral balancing of seismic data." *The Leading Edge* 35, no. 2 (2016): 176-179.

Coleman, J. M., D. B. Prior, and H. H. Roberts. "Geologic development and characteristics of the continental margins, Gulf of Mexico." In *Gulf Coast Association of Geological Societies Transactions*, vol. 36, 1986.

Del Moro, Y., A. Fernandez-Abad, and K. J. Marfurt. "Why should we pay for a merged survey that contains the data we already have? An Oklahoma Redfork example." *The Shale Shaker*, 2013.

Desselle, B. A. "OL P. 2. Frio-Anahuac progradational shoreface and shelf sandstone-Mustang Island and Matagorda Island areas." In *Atlas of Northern Gulf of Mexico Gas and Oil Reservoirs*, vol. 1, 1997, 17-19.

Dondurur, D. *Acquisition and Processing of Marine Seismic Data.* Elsevier, 2018.

Galloway, W. E. "Depositional evolution of the Gulf of Mexico sedimentary basin." In *Sedimentary Basins of the World*, vol. 5, 2008, 505-549.

Gersztenkorn, A., and K. J. Marfurt. "Eigenstructure based coherence computations as an aid to 3D structural and stratigraphic mapping." *GEOPHYSICS* 64, no. 5 (1999): 1468-1479.

Hale, D. "Structure-oriented smoothing and semblance." CWP report 635, 2009.

Höcker, C., and G. Fehmers. "Fast structural interpretation with structure-oriented filtering." *The Leading Edge* 21, no. 3 (2002): 238–243.

Li, Fangyu, and Wenkai Lu. "Coherence attribute at different spectral scales." *Interpretation* 2, no. 1 (2014): SA99-SA106.

Li, Fangyu, et al. "Multispectral coherence." *Interpretation* 6, no. 1 (2018): T61-T69.

Li, F., et al. "Revisit seismic attenuation attributes: Influences of the spectral balancing operation on seismic attenuation analysis." *Interpretation* 9, no. 3 (2021): T767–T779.

Lin, Tengfei, and K. J. Marfurt. "What causes those annoying stair step artifacts on coherence volumes." *AAPG Explorer Geophysical Corner*, March, Article 37830 (2017).

Luo, Y., et al. "Edge-preserving smoothing and applications." *The Leading Edge* 21, no. 2 (2002): 136-158.

Marfurt, K. J. *Seismic Attributes as the Framework for Data Integration Throughout the Oilfield Life Cycle.* Society of Exploration Geophysicists, 2018.

McDonnell, A., M. P. Jackson, and M. R. Hudec. "Origin of transverse folds in an extensional growth-fault setting: Evidence from an extensive seismic volume in the western Gulf of Mexico." *Marine and Petroleum Geology* 27, no. 7 (2010): 1494-1507.

Morse, S., and G. Spear. *Geophysics: Seeing the Whole Picture.* XYZ Publishers, 2022.

Quang, M. T., et al. "Merging of 3D seismic data." *Petrovietnam Journal* 10 (2017): 30-39.

Rangin, C., et al. "Cenozoic gravity tectonics in the northern Gulf of Mexico induced by crustal extension. A new interpretation of multichannel seismic data." *Bulletin de la Société Géologique de France* 179, no. 2 (2008): 117-128.

Spencer, J. A., and E. Barrett. "Exploration History of the Northern Mustang Island, Gulf of Mexico, Texas State Waters." Houston Geological Society Bulletin 50, no. 8 (2007): 22-30.

Swanson, S. M., and A. W. Karlsen. "USGS assessment of undiscovered oil and gas resources for the Oligocene Frio and Anahuac formations, onshore Gulf of Mexico basin." *Search and Discovery*, 101078, USA.

Taner, M. T., F. Koehler, and R. E. Sheriff. "Complex seismic trace analysis." *Geophysics* 44 (1979): 1041-1063.

Tufekčić, D., J. F. Claerbout, and Z. Rašperić. "Spectral balancing in the time domain." *Geophysics* 46, no. 8 (1981): 1182-1188.

Widess, M. B. "How thin is a thin bed?." *Geophysics* 38, no. 6 (1973): 1176-1180.

Worrall, D. M., and S. Snelson. "Evolution of the northern Gulf of Mexico, with emphasis on Cenozoic growth faulting and the role of salt." *AAPG Bulletin* 73, no. 10 (1989): 1237-1257.

APPENDICES

Appendix A: Summary of attributes used in this work

Single trace attributes

Single trace attributes are computed trace by trace, usually in a small vertical data window. In this paper, we use several of the more common single-trace attributes.

- The seismic *amplitude* is simply the processed and migrated data. Amplitude data is a more accurate term than seismic data, which in some way describes all data derived from seismic acquisition and processing.

- The *Hilbert transform* (also called the *quadrature* of the data) is a 90° phase rotated version of the original data (Taner et al., 1979).

- The *envelope* (also called *reflection strength*) is the square root of the squared amplitude and Hilbert transform (Taner et al., 1979).

- The *instantaneous frequency* is the pattern that characterizes a composite reflection. A composite reflection is the composition of individual reflections from a number of closely spaced reflectors that remain nearly constant in acoustic impedance. According to Tanner et al. (1979), the character of a composite reflection changes its frequency response as the sequence of layers changes their thickness. The mathematical definition of this complex seismic trace attribute has been offered in different ways (Barnes, 1992).

Spectral decomposition attributes

Spectral decomposition attributes are also computed trace-by-trace but have earned a category of their own for historical reasons. They may be computed using the short-time Fourier transform (STFT), continuous wavelet transform (CWT), or matching pursuit decomposition

(MPD), among others. We have used several spectral decomposition attributes in this paper using CWT, but not all of them are shown in the figures.

- The *spectral voice* about a given frequency is simply a bandpass-filtered version of the original amplitude volume. For the CWT and MPD methods, the voice is computed by applying a simple Gaussian filter (spectrum of a Morlet wavelet) in the frequency domain to amplitude data (Marfurt, 2018).

- The *spectral magnitude* of a given frequency is the envelope of the spectral voice, which measures the strength of a given spectral component (Marfurt, 2018).

- The *mean frequency* is the spectral-magnitude weighted average of the frequency components and is far more robust than the instantaneous frequency (Marfurt, 2018).

- The *spectral bandwidth i*s the frequency difference between the $1/\sqrt{2}$ upper and lower limits of the magnitude spectrum (or ½ upper and lower limits of the power or square of the magnitude spectrum). The spectral bandwidth is a direct measure of the data spectrum and is far superior to the instantaneous bandwidth that assumes a Gaussian spectrum (Marfurt, 2018).

Geometric attributes

Geometric attributes are computed using a vertical and lateral analysis window (or multitrace template). Like spectral decomposition, there are several ways of computing geometric attributes, including semblance, eigenstructure, and other statistical measures. As with spectral decomposition, I have used several geometric attributes in this paper, not all of which are shown in the figures.

- *Volumetric dip and azimuth* represent the orientation of a local reflector in three dimensions (Marfurt, 2018).

- *Coherence i*s a general term used to describe attributes that measure the continuity of dipping reflectors and, in this work, are always computed along structural dip. I evaluated several alternative coherence algorithms.

  - *Semblance* (also called *variance*) measures the ratio between the energy of the mean trace and the mean energy of each of the traces (Gersztenkorn and Marfurt, 1999).

  - *Energy ratio coherence* measures the ratio of the energy of Karhunen-Loeve (or principal component) filtered version of the data and the energy of the original unfiltered data (Gersztenkorn and Marfurt, 1999; Chopra and Marfurt, 2007).

  - *Sobel filter similarity* measures the ratio of energy of the vector amplitude gradient and the energy of the original unfiltered amplitude data (Luo et al., 1995).

- *Total Energy* is the sum of the squares of each original and Hilbert-transformed sample in the analysis window (Gersztenkorn and Marfurt, 1999).

**Appendix B: Determining the Ormsby wavelet for spectral balancing**

In the application of spectral balancing, the interpreter ideally runs this process twice: a first time to know the spectral voices of their dataset, and a second time applying the most accurate wavelet for their volume according to what was observed in the first step.

In the first computation of spectral balancing in the merged volume, we applied a 0-0-120-120 Hz Ormsby wavelet. With this election, we are making sure that we are capturing all the existing frequencies in the volume. Appendix B. Figure 1 displays the resultant spectral magnitude for the original survey. In general, the result indicates that the more relevant frequencies in this volume (magnitude values above $1x10^5$) are not higher than 60 Hz. We can relate this spectrum with the frequency spectrum analysis shown in Figure 8, in which we see a strong decay of frequencies above 40 Hz. By observing the frequencies with more energy, characterized by the magenta color, we can see how the higher frequencies are in the shallowest areas, while lower frequencies represent the deeper areas (2 seconds and below). After these observations, we conclude that a 5-10-75-85 Hz Ormsby wavelet would capture all the usable frequencies of the data and keep the low energy high frequencies that would contribute to higher detail and resolution to the interpretation.

In the second computing of spectral balancing, we used an Ormsby wavelet with the characteristics mentioned above and obtained the spectra displayed in Appendix B. Figure 2. The first thing to note is that the magnitudes are lower than the original volume; we can tell this by observing a general reduction of magenta color in most of the depths and frequencies. Additionally, we observe the effect of flattening the spectra by taking a depth value, i.e., 1.5 seconds, and seeing how the energy is the same for all the usable ranges of frequencies.
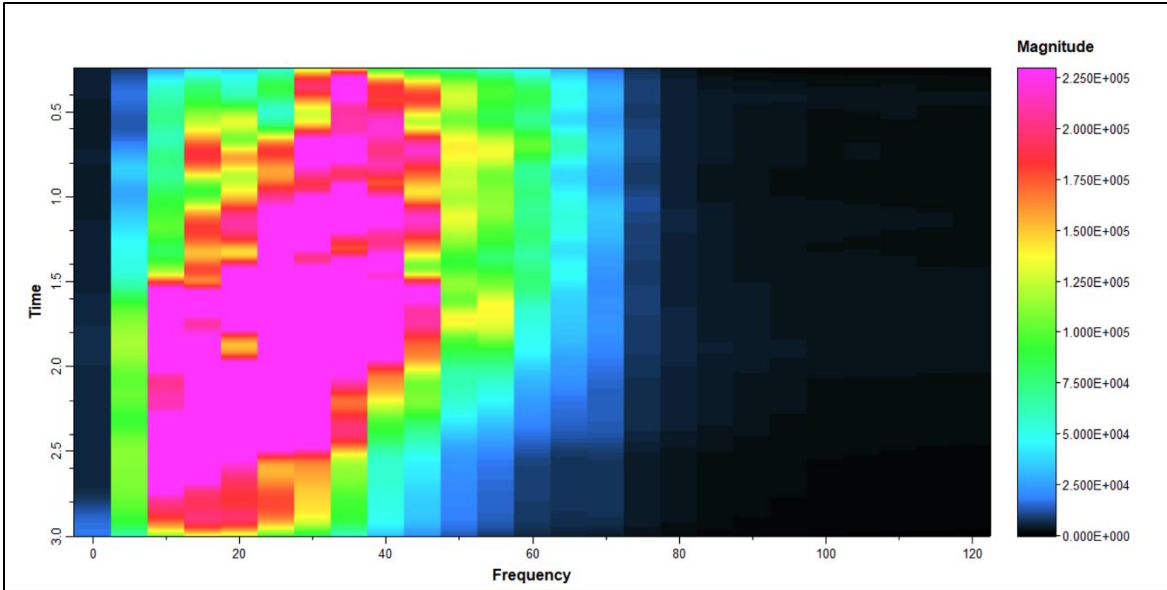
Appendix B. Figure 1. *Spectral magnitude for the original survey. Axe x represents the frequency, with the maximum and minimum values for the selected Ormsby wavelet, and axe y represents the survey time. For depths up to 2 seconds, the higher frequencies are around 45 Hz, and below that time, the maximum frequencies are reduced to 35 Hz and 20 Hz.*
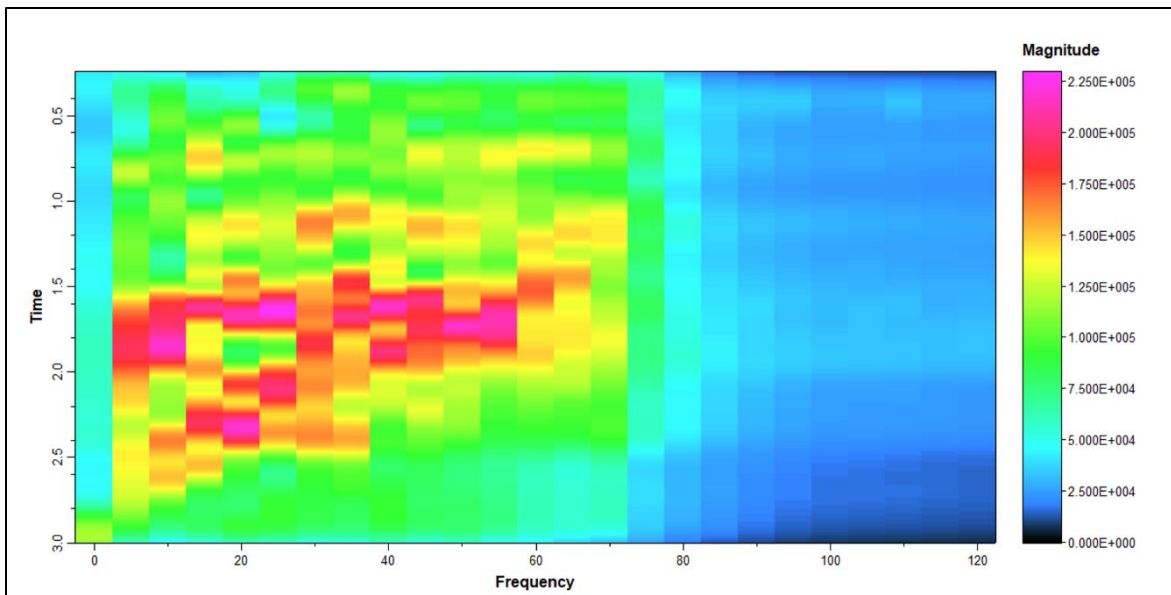

Appendix B. Figure 2. *Spectral magnitude for the original survey. Axe x represents the frequency, with the maximum and minimum values for the selected Ormsby wavelet, and axe y represents the survey time. The figure displays how the final result displays a flattened frequency spectrum in the range of usable frequencies for most of the depths in the volume.*

57

Appendix C: Effects of structured-oriented filtering in the data

This filter smooths the data while preserving the energy in the parallel direction to the structural dip. Additionally, it suppresses random noise and cross-cutting coherent noise. Appendix C. Figure 1 displays the effects of this filter on a cross-section of the volume.
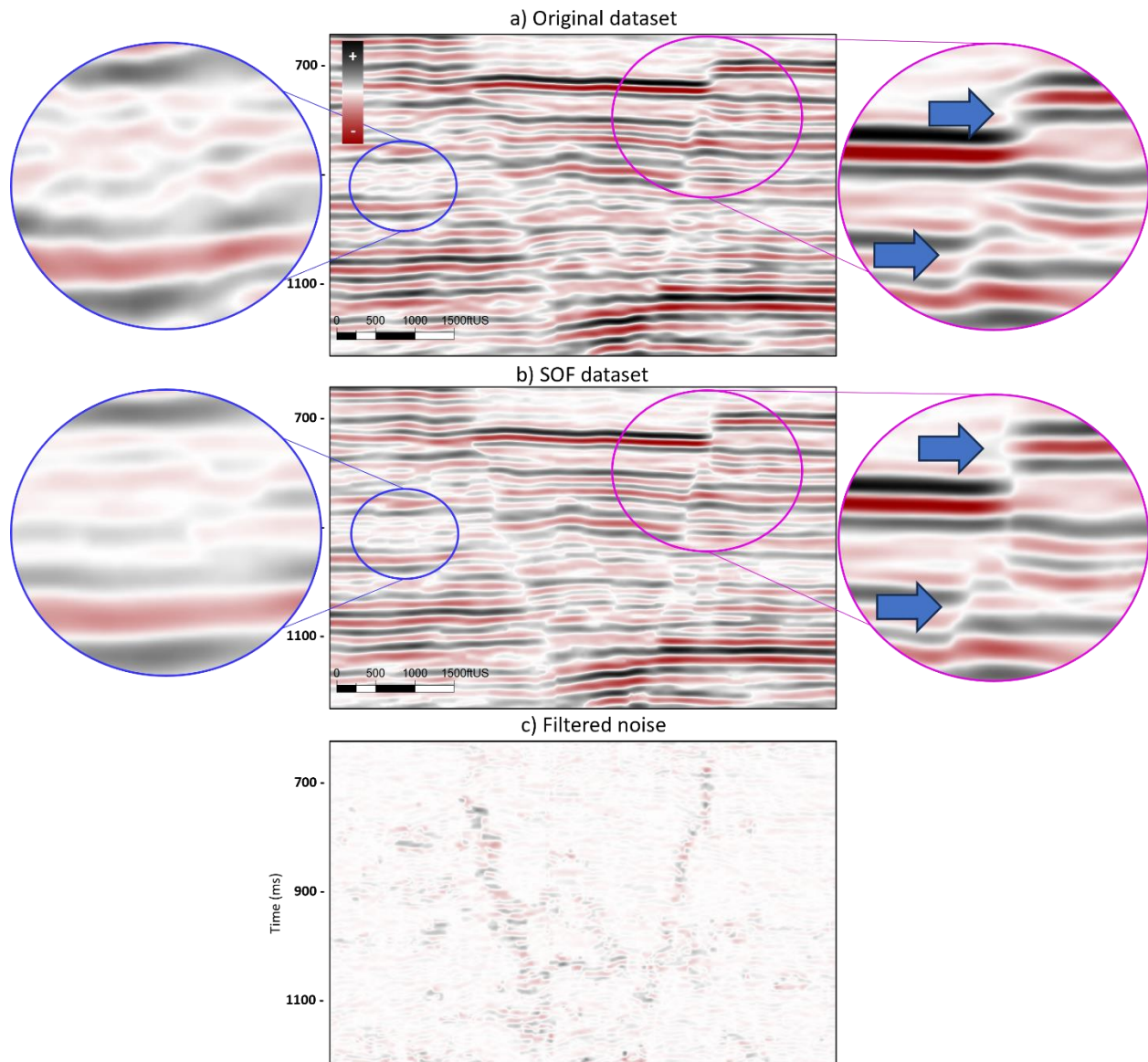

Appendix C. Figure 1. *Cross-section along the a) original seismic dataset, b) structure-oriented filtered (SOF) dataset, and c) the filtered noise obtained after applying SOF to the original volume. The zoomed area in blue displays the effects of smoothing the data, while the magenta sharpens fault planes, as indicated by the blue arrows.*

Appendix D: Tuning frequency of stratigraphic features at z = 932 ms

We use multispectral coherence to understand why we obtained a surprising result where spectral balance harms the visualization of certain features. Multispectral coherence allows us to see the coherence response of a suite of filter banks, and it is useful to identify the frequency at which stratigraphic features and faults are tuned, among others (Li and Lu (2014)). For the case of the Matagorda Island merge volume, we observed that the range of main frequencies goes from 5 to 40 Hz, so we decided to corender the coherence at 20, 30, and 40 Hz to investigate why the stratigraphic edge displayed in Figure 21 is harmed after seismic data conditioning. Appendix D. Figure 1 displays the same correndered time slice at time z = 932 ms that was displayed in the discussion section and additionally displays the correndered coherence at the same time. The red arrow points towards the edge that is visible in the original dataset but surprisingly not visualized after spectral balancing and structured-oriented filtering. In Appendix D. Figure 1-c the same arrow points to a cyan feature, indicating that the stratigraphic edge visible in the original seismic is a feature tuned at 20 Hz. Appendix D. Figure 2 displays two cartoons schematizing the frequency spectrum of the a) original dataset and b) the spectrally balanced and structure-oriented filtered dataset displayed in Figure 8. If we focus on the 20 Hz of the original seismic, we can observe that the original volume has its dominant frequency at this value; for this reason, this dataset does a good job displaying features at that frequency. When looking at the frequency spectrum of the conditioned data, we can observe that the energy to display features at 20 Hz has diminished, demonstrating thus why we are not obtaining an enhanced visualization of some features tuned at that frequency.
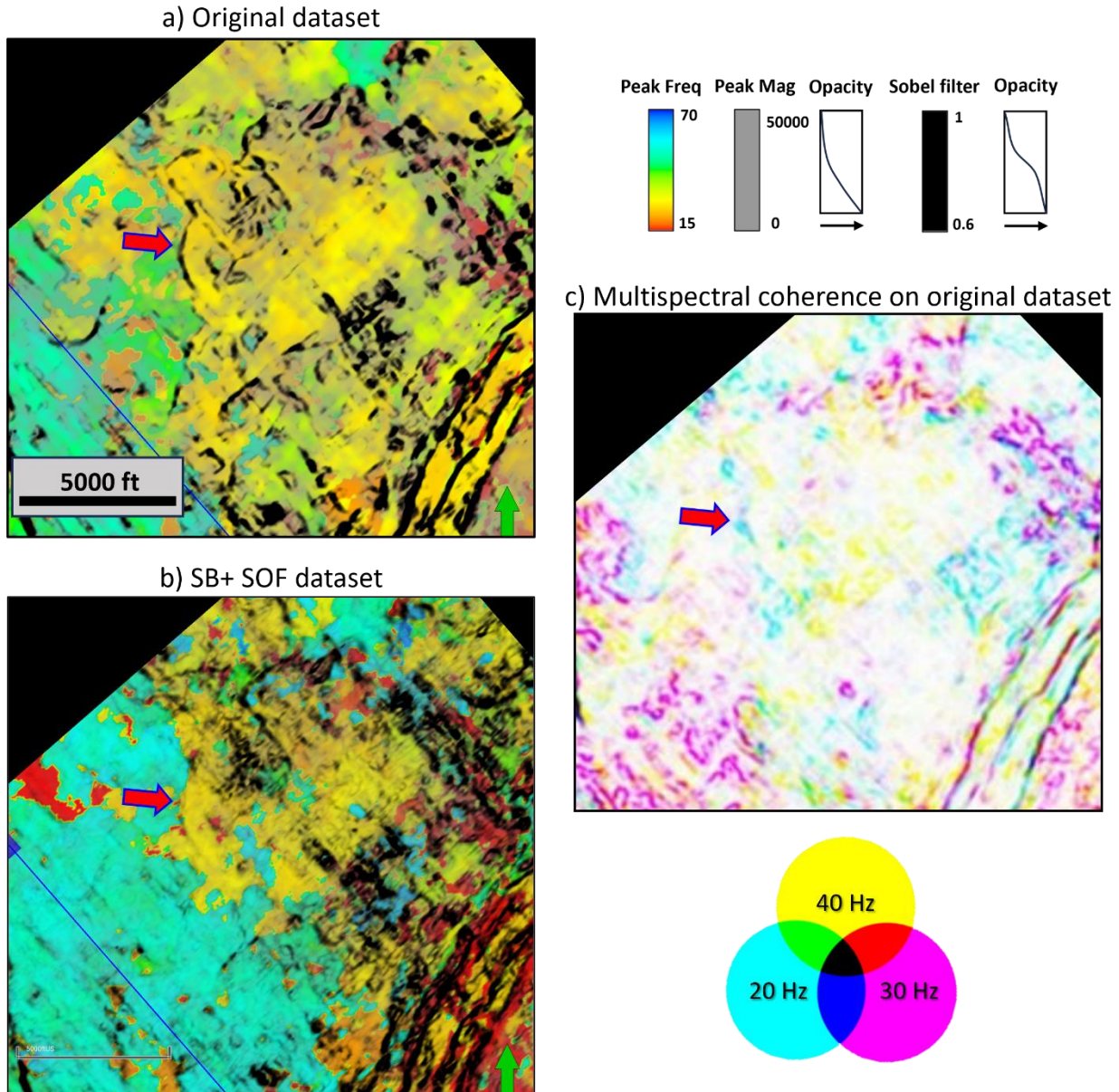
Appendix D. Figure 1. *Zoomed area on stratigraphic edge displaying a corendered time slice at time z = 932 ms displaying peak frequency – peak magnitude – Sobel filter. in a) the original dataset, and b) the spectral balanced and structure-oriented filtered dataset. Figure c) displays the corendered multispectral coherence at 20, 30, and 40 Hz at time z = 932 ms. The arrow in a) points to a stratigraphic edge that is harmed and not visible in b). In Figure c), the same stratigraphic edge is tuned at 20 Hz.*
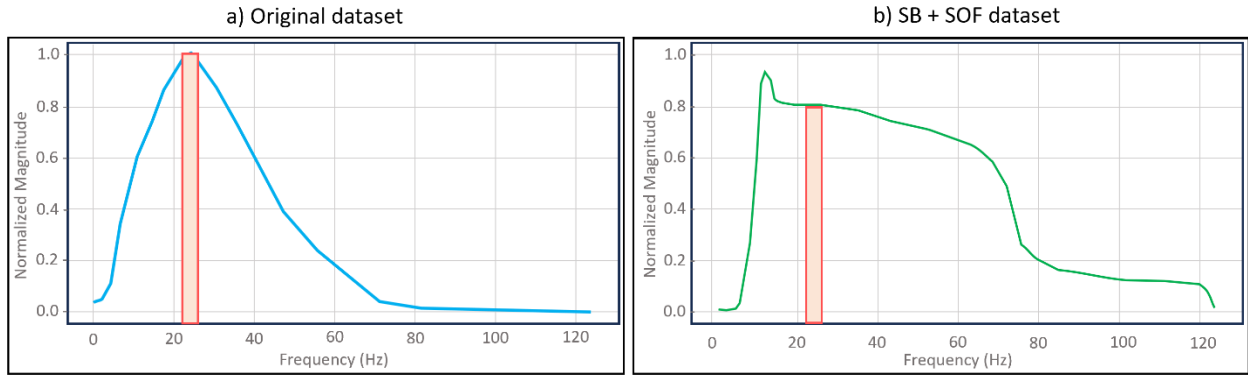
Appendix D. Figure 2. Cartoons schematizing the frequency spectra of the a) original dataset and b) the spectrally balanced and structure-oriented filtered dataset displayed in Figure 8. The orange rectangle allows us to compare how a 20 Hz frequency looks different before and after seismic data conditioning.